Spins of complex fragments in binary reactions and in fission

Horia Pașca

Joint Institute for Nuclear Research, 141980 Dubna, Russia

"Babeș-Bolyai" University , 400084, Cluj-Napoca, Romania

Aim

The description and the prediction of the fission observables

- Charge and mass number of the Compound Nucleus (CN) or of the target and projectile nuclei ;
- Kinetic energy of the projectile;

- Charge and mass distributions of the primary fission fragments (before neutron evaporation);
- Total kinetic energy ;
  - Gives information about the deformations of the fragments
- Excitation energy of the scission configuration;

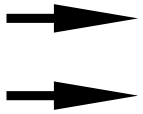

- Neutron multiplicity;
  - Mass of the fission fragments after neutron evaporation;
  - Isotopic distribution;
- Angular momentum of the fission fragments;

Contents

- *Introduction*
- *Description of the model*
- *Results*
- *Discussions:*
  - *Mass and charge distributions*
  - *High excitation energy of the CN*
- *Angular momentum of the fission fragments-results*
  - *Spin components at high bombarding energies*
  - *Spin distribution of heavier systems*
- *Conclusions*

Introduction

- The measured charge (mass) distributions resulting from the fission of pre-actinides are usually symmetric, while the measured charge distributions in the fission of nuclei U-Cf are known to be asymmetric.
- It was suggested that the *competition between symmetric and asymmetric fission is related to the shell effects* in the deformed fissioning nucleus.
  - Experimental data for the high-energy neutron induced fission of ^{238}U shows the conservation of the asymmetric mass distribution, even though the shell effects are supposed to be completely dampened.
  - Also in neutron-deficient ^{180}Hg the *asymmetric mass distribution* of fission fragments was unexpectedly observed in recent experiment *[2-4].*
  - The new experimental data of fission of ^{180}Hg show that the asymmetric mass distribution cannot be anticipated only from the microscopic effects in the fragments alone.

- The experimental angular momentum distributions of the fission fragments are lower than the calculated ones at large charge/mass asymmetry.
  - Also, the variance of these distributions can not be accounted for at large asymmetry, even taking into account the angular momentum bearing modes.

- We have shown in recent studies [5-8] that the fission observables are related to the combined energy dependent structures in the PESs.

[1] U. Brosa, S. Grossmann, and A. Muller, Phys. Rep. ***197****, 167 (1990).*
[2] A.N. Andreyev, M. Huyse, and P. Van Duppen, Rev. Mod. Phys. ***85****, 1541 (2013).*
[3] K.-H. Schmidt et al., Nucl. Phys. A ***665****, 221 (2000); K.-H. Schmidt et al., Nucl. Phys. A* ***693****, 169 (2001).*
[4] A.N. Andreyev et al., Phys. Rev. Lett. ***105****, 252502 (2010).*
[5] H. Pașca, A.V. Andreev , G.G. Adamian , N.V. Antonenko, and Y. Kim, Phys. Rev. C ***93****, 054602 (2016)*
[6] H. Pașca, A.V. Andreev, G.G. Adamian, and N.V. Antonenko, Phys. Rev. C ***94****, 064614 (2016)*
[7] H. Pașca, A.V. Andreev, G.G. Adamian, and N.V. Antonenko, Phys. Lett. B ***760****, 800 (2016).*
[8] H. Pașca, A.V. Andreev, G.G. Adamian, and N.V. Antonenko, Eur. Phys. J. A ***52****, 369 (2016).*

Model

Parameters Z_1, A_1, β_1, β_2 and R completely describe the geometry of the system.

The interaction potential between the fragments is:

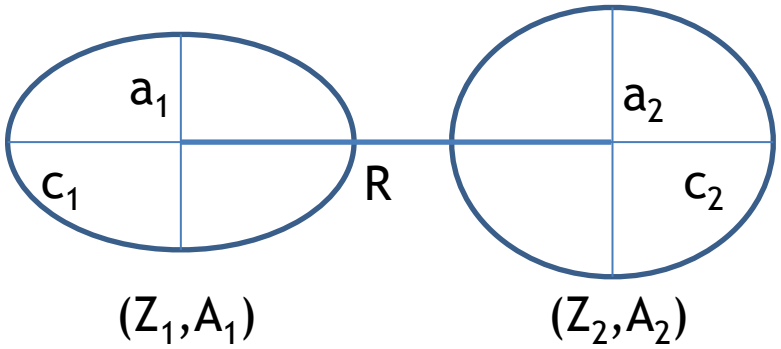

$$V(R, Z, A, J, \beta_1, \beta_2) = V_N + V_C$$

$$V_c(R, Z_1, Z_2, \beta_1, \beta_2) = \frac{e^2 Z_1 Z_2}{R} + \left(\frac{9}{20\pi}\right)^{1/2} \frac{e^2 Z_1 Z_2}{R^3} \sum_{i=1}^{2} R_i^2 \beta_i \left[1 + \frac{2}{7}\left(\frac{5}{\pi}\right)^{1/2} \beta_i\right] P_2(cos\theta_i)$$

$$V_N = \int \rho_1(r_1)\rho_2(R - r_2)F(r_1 - r_2)dr_1 dr_2$$

$$F(r_1 - r_2) = C_0[F_{in}\frac{\rho_1(r_1)}{\rho_{00}} + F_{ex}(1 - \frac{\rho_1(r_1)}{\rho_{00}})]\delta(r_1 - r_2)$$

$$\rho_0(r) = \rho_1(r) + \rho_2(R - r)$$

$$F_{in,ex} = f_{in,ex} + f'_{in,ex}\frac{(N - Z)(N_2 - Z_2)}{(N + Z)(N_2 + Z_2)}$$

$$C_0 = 300 MeV fm^3$$

$$f_{in} = 0.09, f_{ex} = -2.59$$

$$\rho_{00} = 0.17 fm^{-3}, a = 0.51 - 0.56 fm$$

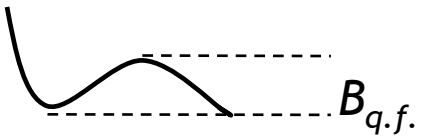

Sh. A. Kalandarov, G.G. Adamian, N.V. Antonenko, W. Scheid, Phys. Rev. C 82, 044603 (2010)

Model

- *The total energy:*

$$U(A_i, Z_i, \beta_i, d) =$$
$$= U_{macro}(A_i, Z_i, \beta_i, d) + \delta U^{shell}(A_i, Z_i, \beta_i) =$$
$$= \sum_{i=1,2} U_i^{LD}(A_i, Z_i, \beta_i) + \sum_{i=1,2} \delta U_i^{shell}(A_i, Z_i, \beta_i', E_i^*) +$$
$$+ V_N(A_i, Z_i, \beta_i, d) + V_C(A_i, Z_i, \beta_i, d).$$

$$U_i^{L.D.}(A_i, Z_i, \beta_i) = U_i^{Surface}(A_i, Z_i, \beta_i) + U_i^{C}(A_i, Z_i, \beta_i) + U_i^{Sym}(A_i, Z_i)$$

- *Liquid drop terms:*

$$U_i^{sym}(A_i, Z_i) = 27.612 \frac{(N_i - Z_i)^2}{A_i}$$

$$U_i^{C}(A_i, Z_i, \beta_i) = \frac{3}{5} \frac{(Z_i e)^2}{R_{0,i}} \frac{\beta_i^{1/3}}{\sqrt{\beta_i^2 - 1}} ln(\beta_i + \sqrt{\beta_i^2 - 1})$$

$$U_i^{Surface}(A_i, Z_i, \beta_i) = \sigma_i S_i$$

$$\sigma_i = \sigma_{0,i}(1 + k_i(\beta_i - \beta_i^{g.s.})^2)$$

$$\sigma_{0,i} = 0.9517(1 - 1.7826((N_i - Z_i)^2)/A_i)^2)$$

$$k_i = \frac{1}{1 + exp[-0.063(C_{vib}(Z_i, A_i) - 67)]}$$

$$C_{vib}(Z_i, A_i) = \frac{\hbar \omega_{vib}^i (3 Z_i e R_{0,i}^2/(4\pi))^2}{2 B(E2)_{vib}^i}$$

$$B(E2)_{vib} = E_{2^+}^i B(E2)_{rot}^i / (\hbar \omega_{vib}^i)$$

J. Maruhn and W. Greiner, Z. Phys. ***251****, 431 (1972).*

Model

Excitation energy: of the scission configuration can be calculated as a sum of the initial excitation energy of the fissioning nucleus and the difference of the potential energies of the fissioning nucleus and scission configuration:

$$E^*(A_i, Z_i, \beta_i, R_m) = E^*_{CN} + [U_{CN}(A, Z, \beta) - U(A_i, Z_i, \beta_i, R_m)] .$$

$$T_{DNS}(E^*) = \sqrt{E^*/a} \ , a = A/12\, MeV^{-1}$$

Shell damping:

$$\delta U_i^{shell}(A_i, Z_i, \beta_i', E_i^*) = \delta U_i^{shell}(A_i, Z_i, \beta_i', E_i^* = 0) exp[-E_i^*/E_D]$$

Temperature dependence of LD terms:

$$U_i^{sym}(A_i, Z_i, T) = U_i^{sym}(A_i, Z_i, T = 0)(1 + 6 * 10^{-4} E_i^*/A_i),$$

$$U_i^{C}(A_i, Z_i, \beta_i, T) = U_i^{C}(A_i, Z_i, \beta_i, T = 0)(1 - 0.12 E_i^*/A_i)$$

$$U_i^{Surf}(A_i, Z_i, \beta_i, T) = U_i^{Surf}(A_i, Z_i, \beta_i, T = 0)(1 + 0.102 E_i^*/A_i).$$

$$k_i(E_i^*) = k_i * exp\,[-E_i^*/E_k]$$

*G. Sauer, H. Chandra, U. Mosel, Nucl. Phys. A **264** (1976) 221-243*

Model

Yields:

Using $P_{Z,A}(E^*_{CN}, \beta_1, \beta_2) \sim exp\{-U(R_m, Z, A, \beta_1, \beta_2)/T\}$

$P^{decay}_{Z,A,\beta_1,\beta_2} \sim exp\{-B_{qf}(Z, A, \beta_1, \beta_2)/T\}$

$$w(A_i, Z_i, \beta_i, E^*) = N_0 exp[-\frac{U(A_i, Z_i, \beta_i, R_m) + B_{qf}(A_i, Z_i, \beta_i)}{T}]$$

The different yields can be calculate by integrating over the deformations:

$$Y(A_i, Z_i) = N_0 \int\int w(A_i, Z_i, \beta_1, \beta_2, E^*)\, \mathrm{d}\beta_1 \mathrm{d}\beta_2,$$

$$Y(A_i) = N_0 \sum_{Z_i} \int\int w(A_i, Z_i, \beta_1, \beta_2, E^*)\, \mathrm{d}\beta_1 \mathrm{d}\beta_2,$$

$$Y(Z_i) = N_0 \sum_{A_i} \int\int w(A_i, Z_i, \beta_1, \beta_2, E^*)\, \mathrm{d}\beta_1 \mathrm{d}\beta_2,$$

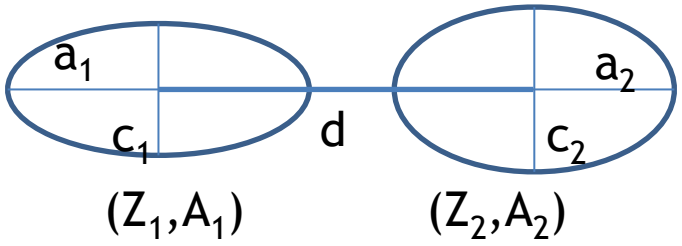

$$TKE(A_i, Z_i) = V_c(A_i, Z_i, \beta_1, \beta_2) + V_n(A_i, Z_i, \beta_1, \beta_2)$$

$$<TKE>(A_i) = \frac{\sum_{Z_i} \int TKE(A_i, Z_i, \beta_1, \beta_2)\, w(A_i, Z_i, \beta_1, \beta_2, E^*) d\beta_1 d\beta_2}{\sum_{Z_i} \int w(A_i, Z_i, \beta_1, \beta_2, E^*) d\beta_1 d\beta_2}$$

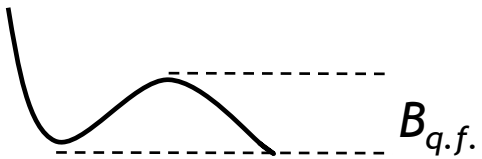

Model

- Because the dynamical treatment is not explicitly performed here, we "simulate" the dynamical effects by *restricting the minimum value of the quasifission barrier*.

- In the calculations, we take into consideration only those configurations for which B_{qf} is larger than z~ 1 MeV.

  — This condition restricts the highly deformed configurations in the (β_1, β_2) plane and, correspondingly, restricts the upper limits of integration over deformations.

$$Y(A_i, Z_i) = N_0 \int\int W(A_i, Z_i, \beta_1, \beta_2, E^*)\, \mathrm{d}\beta_1 \mathrm{d}\beta_2$$

Model

The angular momentum of fission fragments (due to orbital motion)

- If the condition of long interaction times is satisfied, the system attains equilibrium which corresponds to rigid rotation, characterized by matching the orbital and intrinsic angular velocities.
  - The angular momenta of one of the nuclei after break-up is given by:

$$I_i = \frac{\Im_i}{\Im_1 + \Im_2 + \mu r^2} I_0$$

Fission reactions with heavy ions

Orbital spin component

The production cross sections:

$$\sigma_{Z,A}(E_{c.m.}) = \sum_{J=0}^{J_{max}} \sigma_{cap}(E_{c.m.}, J) W_{Z,A}(E^*_{CN}, J)$$

$$\sigma_Z(E_{c.m.}) = \sum_A \sigma_{Z,A}(E_{c.m.}, J)$$

$$\sigma_A(E_{c.m.}) = \sum_Z \sigma_{Z,A}(E_{c.m.}, J)$$

The capture cross section:

$$\sigma_{cap}(E_{c.m.}, J) = \pi\lambda^2(2J+1)P_{cap}(E_{c.m.}, J)$$

$\lambda^2 = \hbar^2/2\mu E_{c.m.}$ is the reduced de Broglie wavelength

$$P_{cap}(E_{c.m.}, J) = (1 + exp\{2\pi[V(R_b, Z_i, A_i, J=0) + \\ + (\hbar^2 J(J+1))/(2\mu R_b^2(J=0)) - E_{c.m.}]/\hbar\omega\})^{-1}$$

Hill-Wheeler formula.

Orbital spin component

The average angular momentum is then:

$$\sigma_{Z,A}(E_{c.m.}) = \sum_{J=0}^{J_{max}} \sigma_{cap}(E_{c.m.}, J) W_{Z,A}(E^*_{CN}, J) \overset{\wedge}{\vec{\nu}}$$

$$< J >_{Z,A} = \frac{\sum_{J=0}^{J_{max}} J\sigma_{Z,A}(E_{c.m.}, J)}{\sum_{J=0}^{J_{max}} \sigma_{Z,A}(E_{c.m.}, J)}$$

$$I_{Z_i,A_i} = \frac{\Im_i}{\Im_1 + \Im_2 + \mu R_m^2} \frac{\sum_{J=0}^{J_{max}} J\sigma_{Z_i,A_i}(E_{c.m.}, J)}{\sum_{J=0}^{J_{max}} \sigma_{Z_i,A_i}(E_{c.m.}, J)}.$$

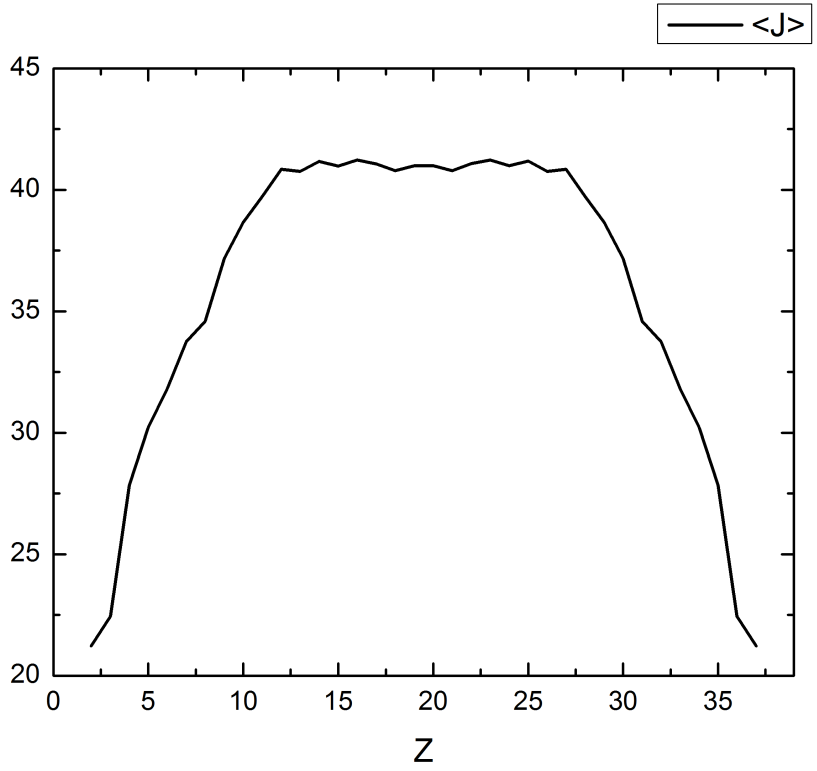

Average angular momentum (in units of ħ) of the DNS in the exit channel calculated for the 166 MeV ^{20}Ne+^{63}Cu reaction.

H. Pașca, Sh. Kalandarov, G.G. Adamian, and N.V. Antonenko, *"Spins of complex fragments in binary reactions within dinuclear system model"*, sent to Phys. Rev. C.

Orbital spin component

- The interaction potential:

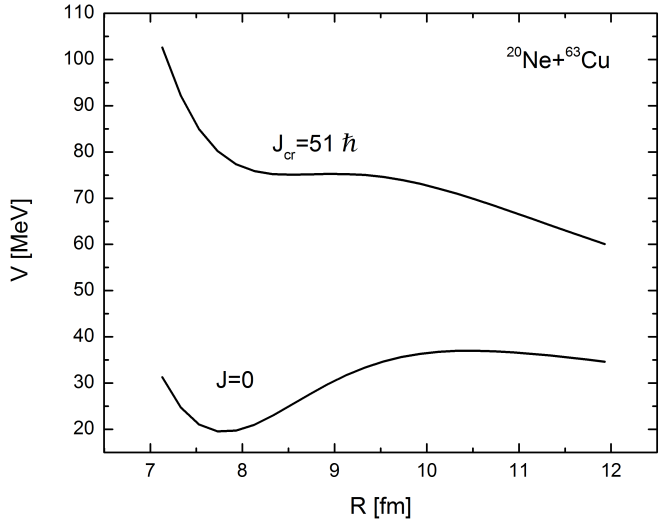

H. Pașca, Sh. Kalandarov, G.G. Adamian, and N.V. Antonenko, *"Spins of complex fragments in binary reactions within dinuclear system model"*, sent to Phys. Rev. C.

- The maximum value for the angular momentum J_{max} is limited by the value of the critical or of the kinematic angular momentum

$$J_{kin} = \sqrt{2\mu[E_{c.m.} - V(R_b, Z_i, A_i, J = 0)]}R_b/\hbar$$

depending on which one is smaller.

$$R_m \sim R_1[1 + \sqrt{5/(4\pi)}\beta_1] + R_2[1 + \sqrt{5/(4\pi)}\beta_2] + 0.5fm$$

$$R_b \sim R_m + 2fm$$

Sh. A. Kalandarov, G.G. Adamian, N.V. Antonenko, W. Scheid, Phys. Rev. C 82, 044603 (2010)

Variances

From orbital motion

$$< J >_{Z_i,A_i} = \frac{\sum_{J=0}^{J_{max}} J\sigma_{cap}(E_{c.m.},J)W_{Z_i,A_i}(E^*_{CN},J)}{\sum_{J=0}^{J_{max}} \sigma_{cap}(E_{c.m.},J)W_{Z_i,A_i}(E^*_{CN},J)}$$

$$< J^2 >_{Z_i,A_i} = \frac{\sum_{J=0}^{J_{max}} J(J+1)\sigma_{cap}(E_{c.m.},J)W_{Z_i,A_i}(E^*_{CN},J)}{\sum_{J=0}^{J_{max}} \sigma_{cap}(E_{c.m.},J)W_{Z_i,A_i}(E^*_{CN},J)}$$

$$\sigma_{Z_i,A_i} = \frac{\Im_i}{\Im_1 + \Im_2 + \mu R_m^2}\sqrt{< J^2 >_{Z_i,A_i} - < J >^2_{Z_i,A_i}}$$

From the angular momentum bearing modes:

- Bending $\sigma^2_{Bending} = (|a_{1B}| + a_{2B})^2\tau$
- Twisting $\sigma^2_{iTwisting} = a^2_{iTw}\left(1 - \frac{2}{\pi}\right)\tau$

$$\tau = \frac{\sum_{J=0}^{J_{max}} T_{DNS}(J)\sigma_{Z,A}(E_{c.m.},J)}{\sum_{J=0}^{J_{max}} \sigma_{Z,A}(E_{c.m.},J)}$$

R.P.Schmitt, A.J.Pacheco, Nucl.Phys. A379, 313 (1982)

Results - charge distributions in the electromagnetic induced fission

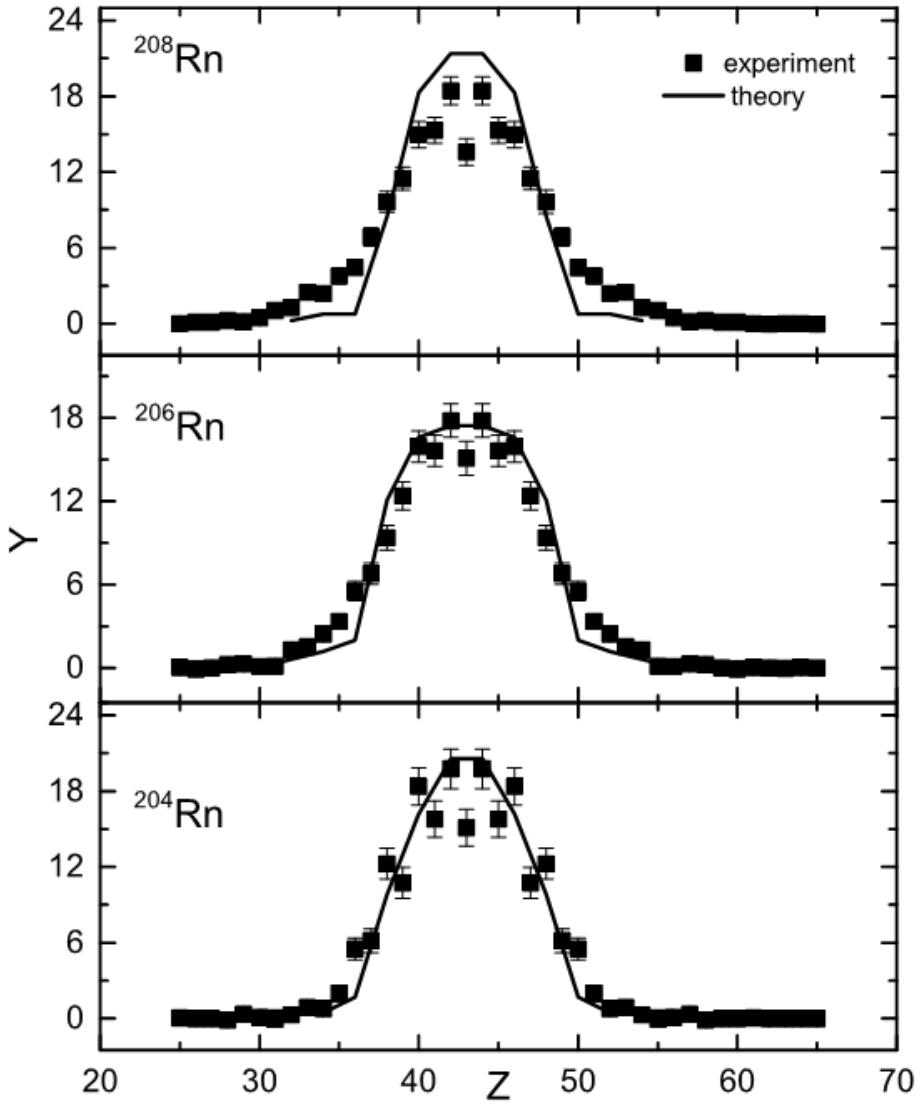

The calculated charge distributions (lines) for the electromagnetic-induced fission of $^{204\text{-}208}$Rn.

*H. Pașca, A.V. Andreev, G.G. Adamian, and N.V. Antonenko, Phys. Lett. B **760**, 800 (2016).*
Experimental data taken from: K.-H. Schmidt *et al.*, Nucl. Phys. A 665, 221 (2000);

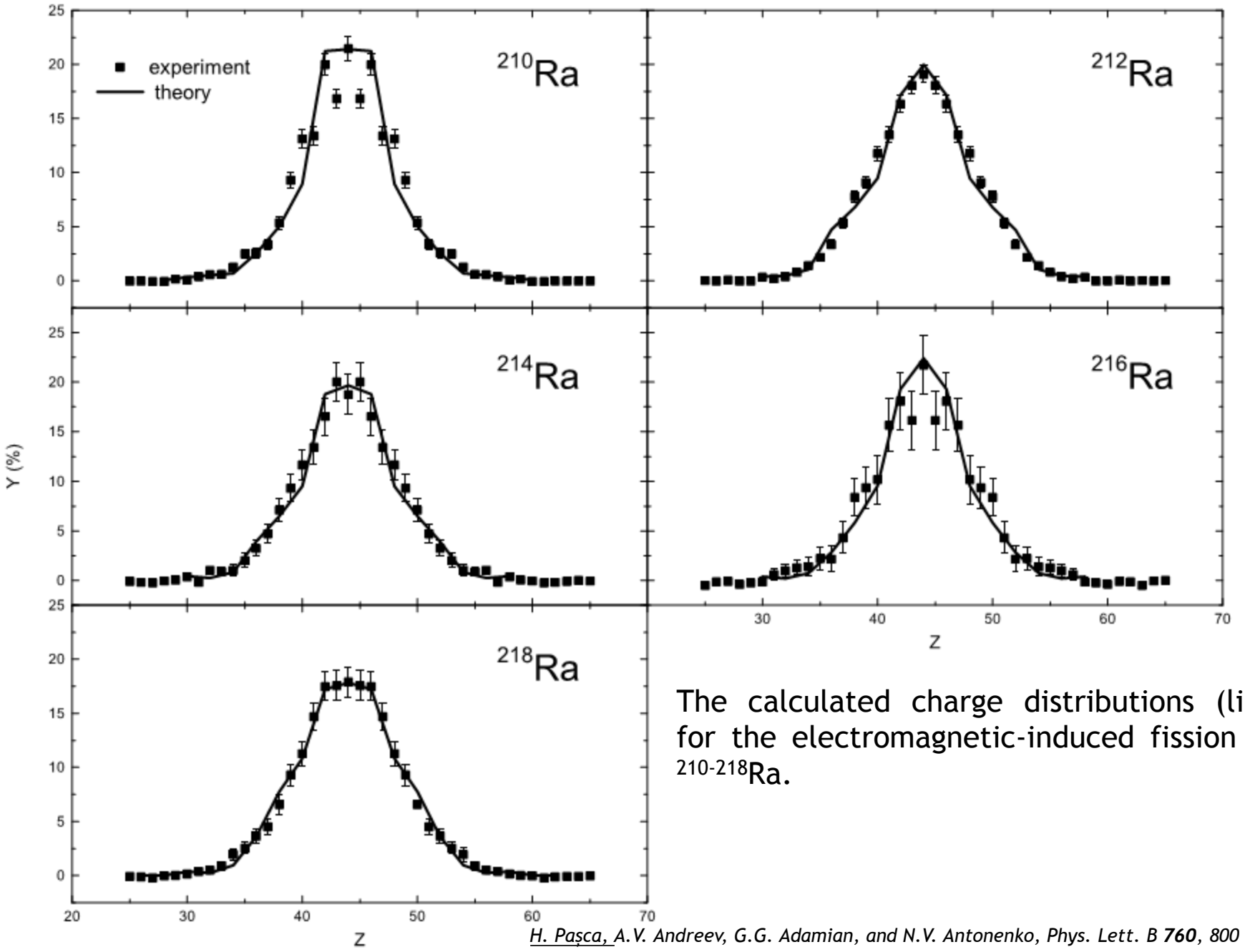

The calculated charge distributions (lines) for the electromagnetic-induced fission of $^{210\text{-}218}$Ra.

*H. Pașca, A.V. Andreev, G.G. Adamian, and N.V. Antonenko, Phys. Lett. B **760**, 800 (2016).*
Experimental data taken from: K.-H. Schmidt *et al.*, Nucl. Phys. A 665, 221 (2000);

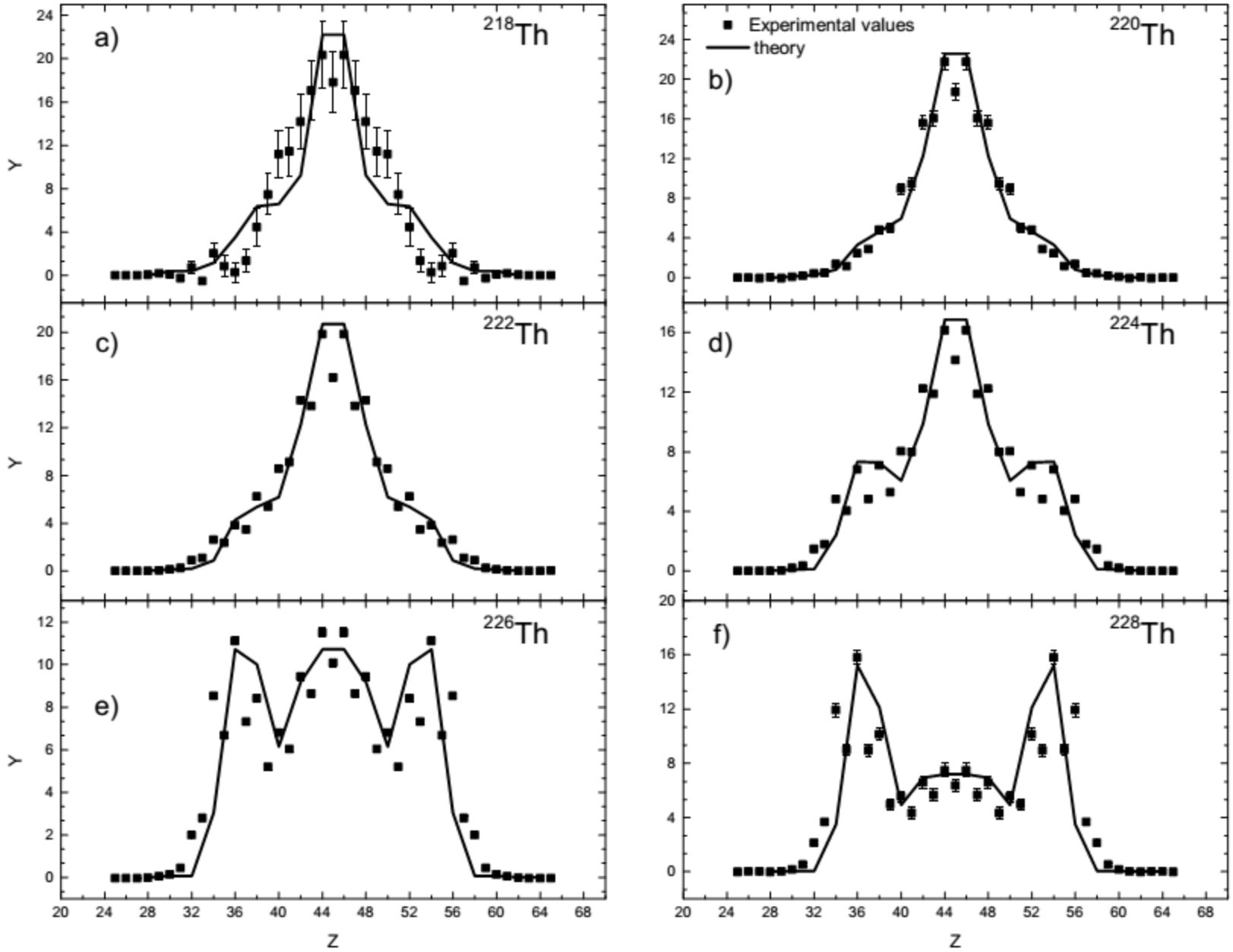

The calculated charge distributions (lines) for the electromagnetic-induced fission of $^{218\text{-}228}$Th.

*H. Pașca, A.V. Andreev, G.G. Adamian, and N.V. Antonenko, Phys. Lett. B **760**, 800 (2016).*
Experimental data taken from: K.-H. Schmidt *et al.*, Nucl. Phys. A 665, 221 (2000);

Results

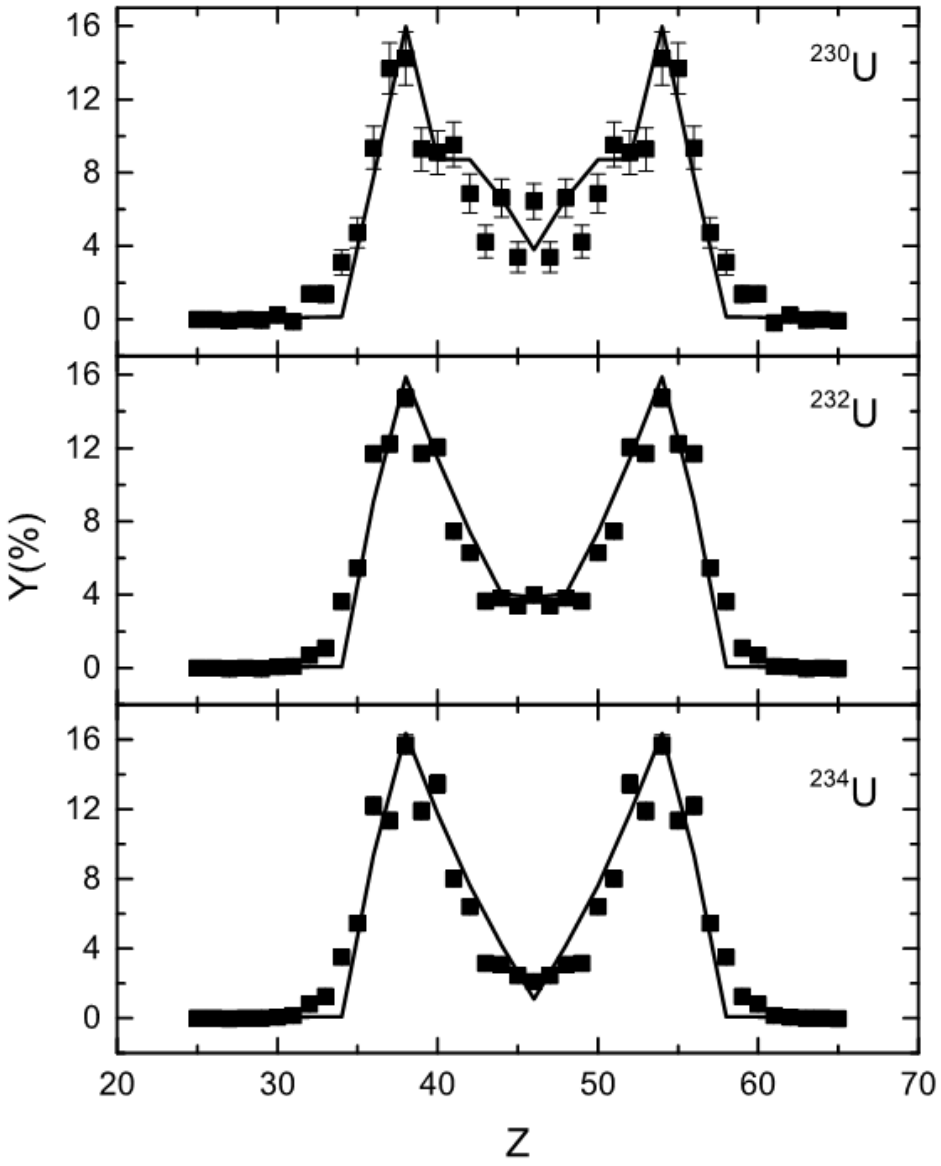

The calculated charge distributions (lines) for the electromagnetic-induced fission of $^{230\text{-}234}$U.

Our model is well suited for describing both asymmetric and symmetric fission distributions as well as the transition between the two.

*H. Pașca, A.V. Andreev, G.G. Adamian, and N.V. Antonenko, Phys. Lett. B **760**, 800 (2016).*
Experimental data taken from: K.-H. Schmidt *et al.*, Nucl. Phys. A 665, 221 (2000);

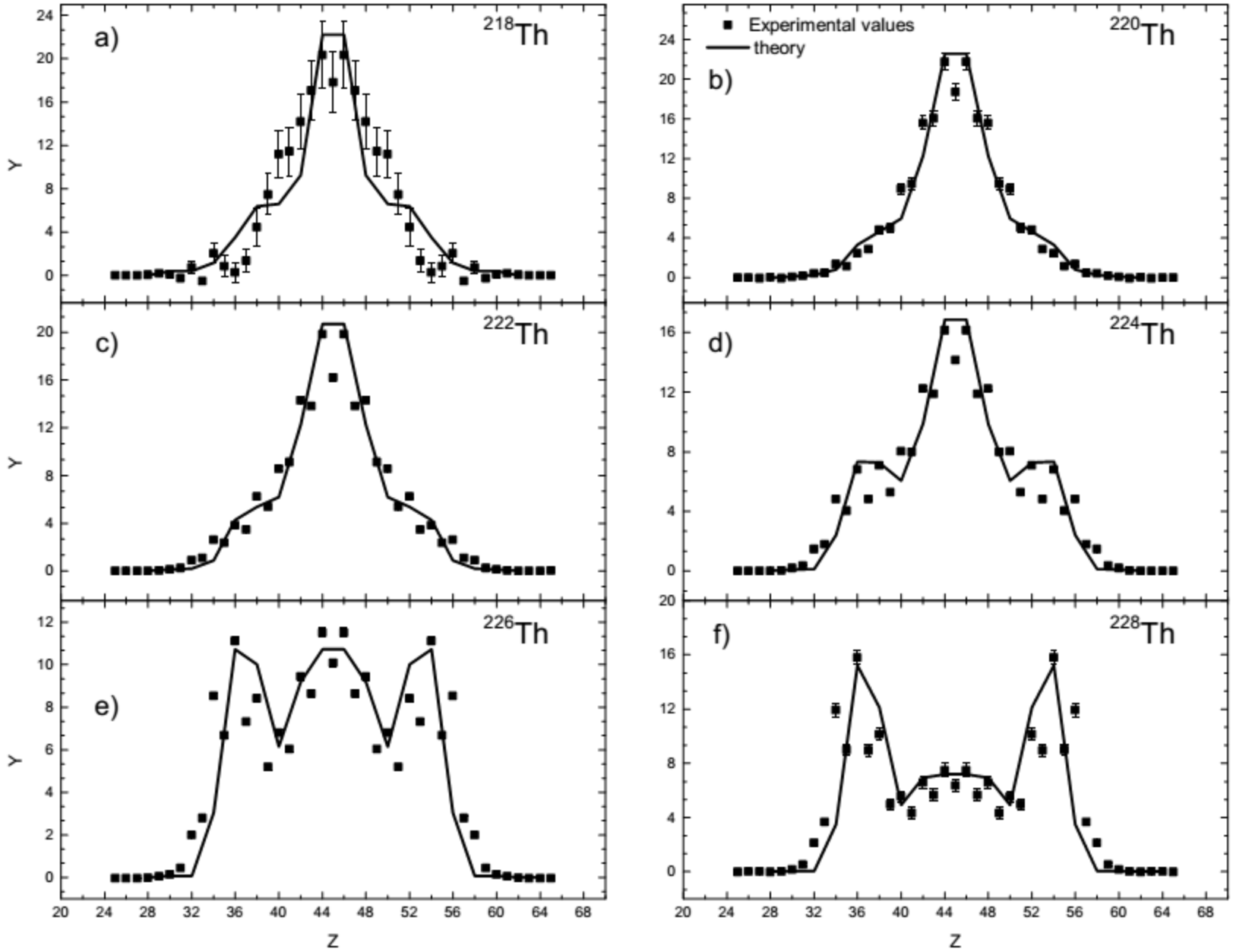

The calculated charge distributions (lines) for the electromagnetic-induced fission of $^{218\text{-}228}$Th.

Experimental data taken from: K.-H. Schmidt *et al.*, Nucl. Phys. A 665, 221 (2000);

Results

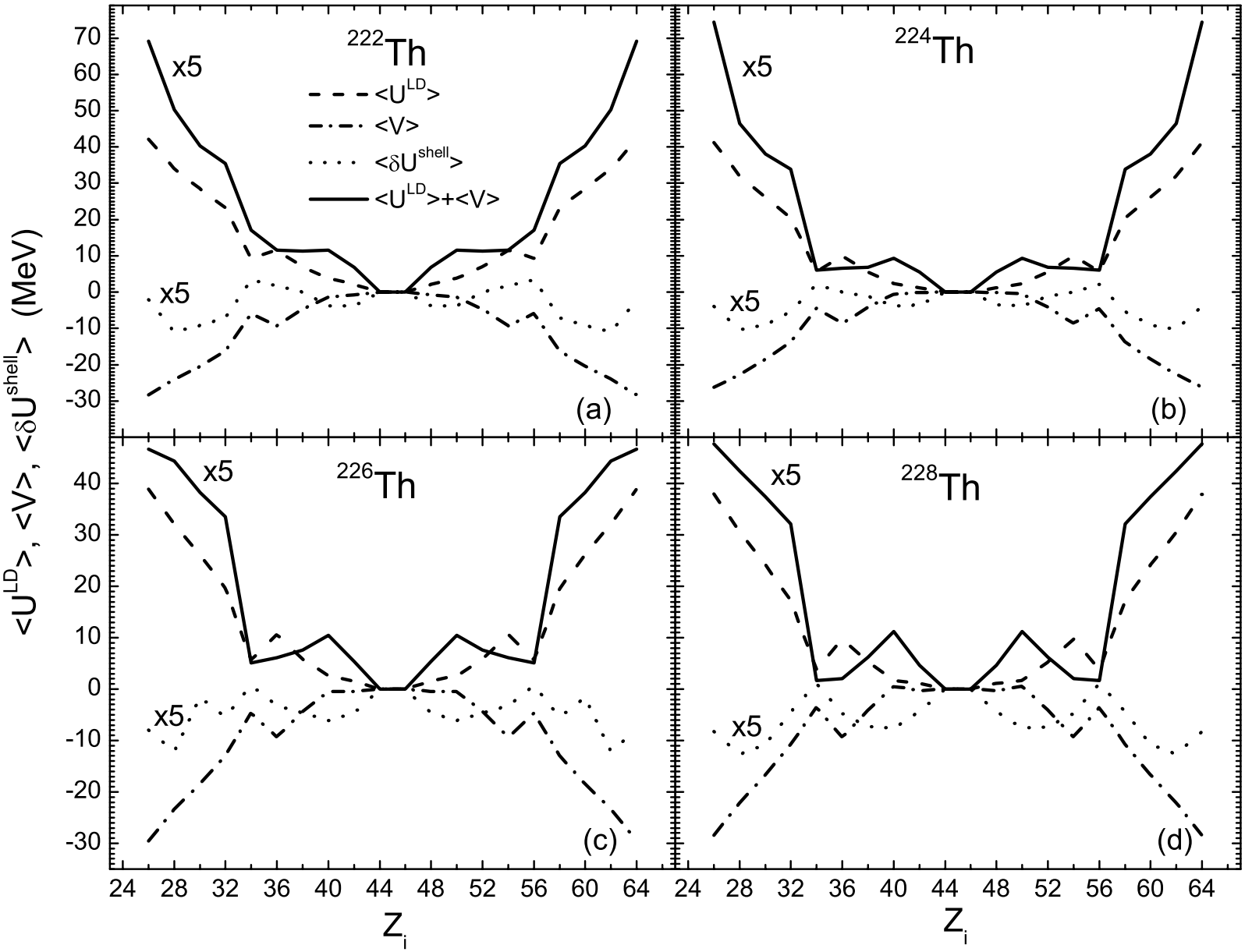

<Shells> and <LDM>+<Vint> values were multiplied by a factor of 5.

H. Pașca, A.V. Andreev, G.G. Adamian, and N.V. Antonenko, Eur. Phys. J. A ***52****, 369 (2016).*

Results

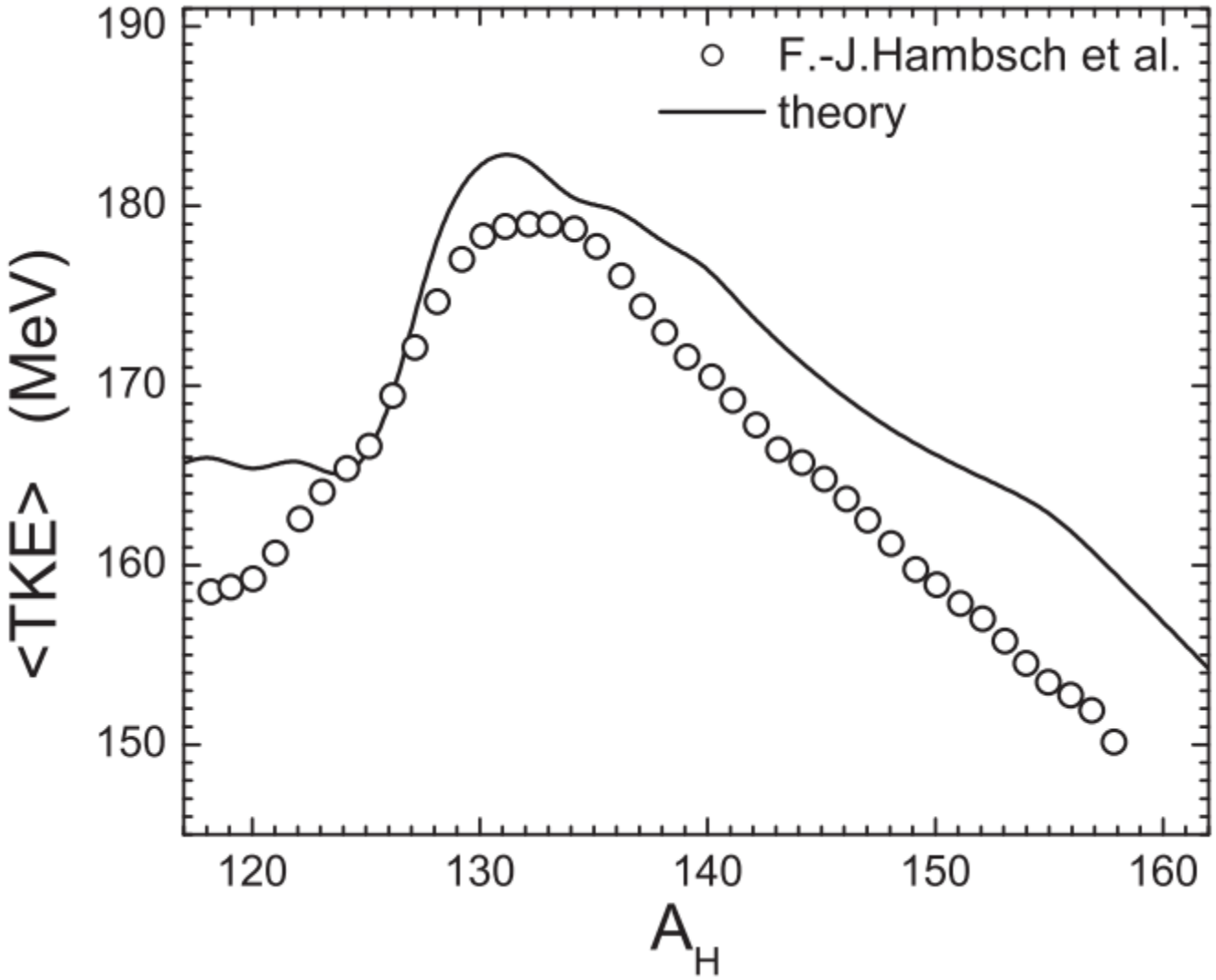

Calculated TKE distribution compared with experimental data for the $^{235}U(n_{thermal}, f)$ reaction.

***H. Pașca**, A.V. Andreev, G.G. Adamian , N.V. Antonenko, Phys. Rev. C **93**, 054602 (2016)*

Experimental data taken from:

- Ch. Straede, C. Budtz-Jorgensen, and H.-H. Knitter, Nucl. Phys.
- A **462**, 85 (1987); F.-J. Hambsch, H.-H. Knitter, and C. BudtzJorgensen, *ibid.* **491**, 56 (1989)

Discussions – High excitation energy of the CN

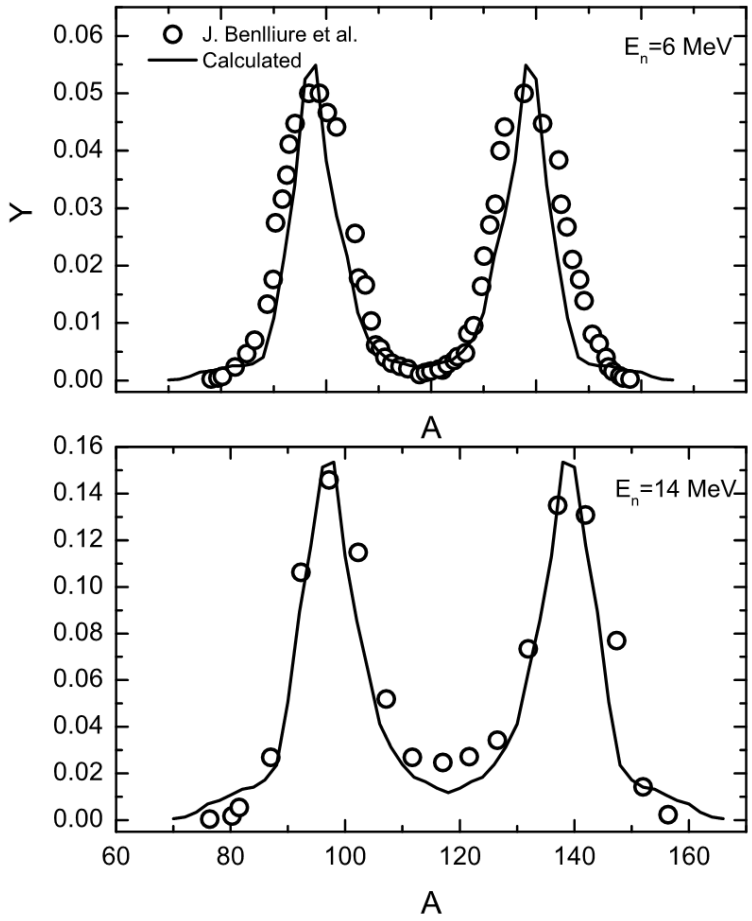

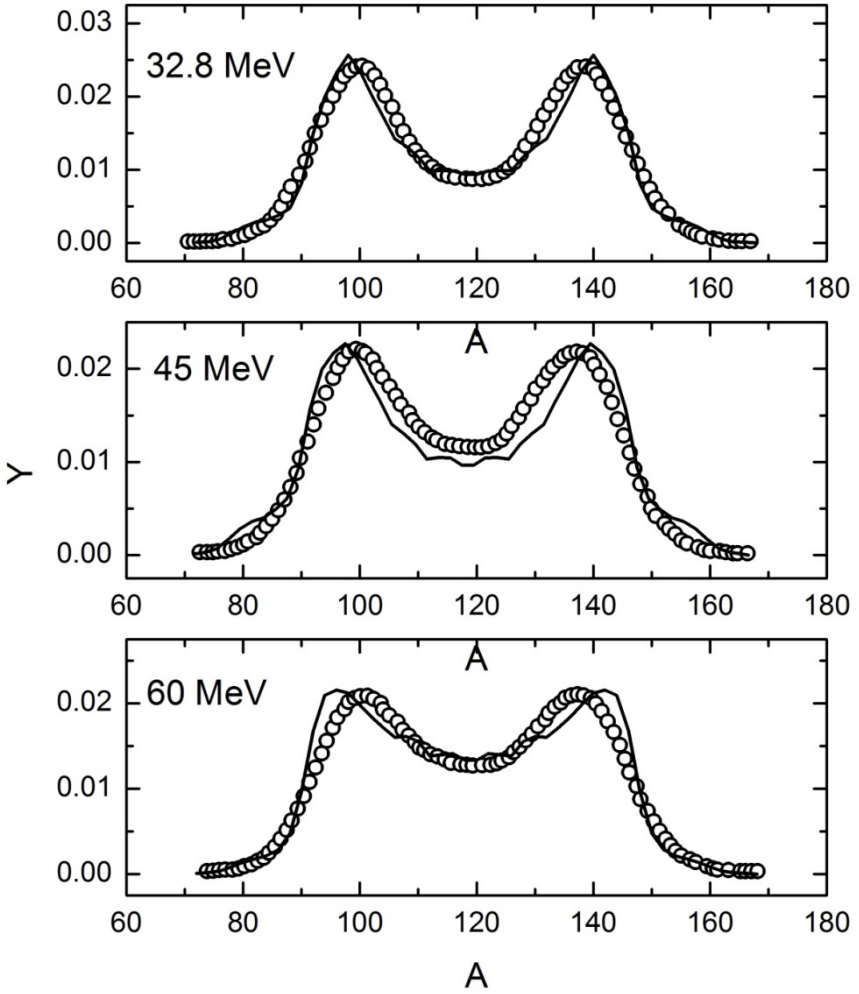

Left: The calculated mass distributions (lines) for fission of ^{235}U by neutron with incident energies 6 MeV (upper part) and 14 MeV (lower part).

Right: The calculated fragment mass distributions in the $^{238}U(n,f)$ reactions at the indicated incident neutron energies.

Experimental data taken from:

- J. Benlliure et al. / Nucl Phys A 628 (1998) 458-478
- Ch. Straede et. al., Nucl. Phys. A 462 (1987) 129
- I. V. Ryzhov et. Al. , Phys Rev C83 054603 (2011)

Discussions – High excitation energy of the CN

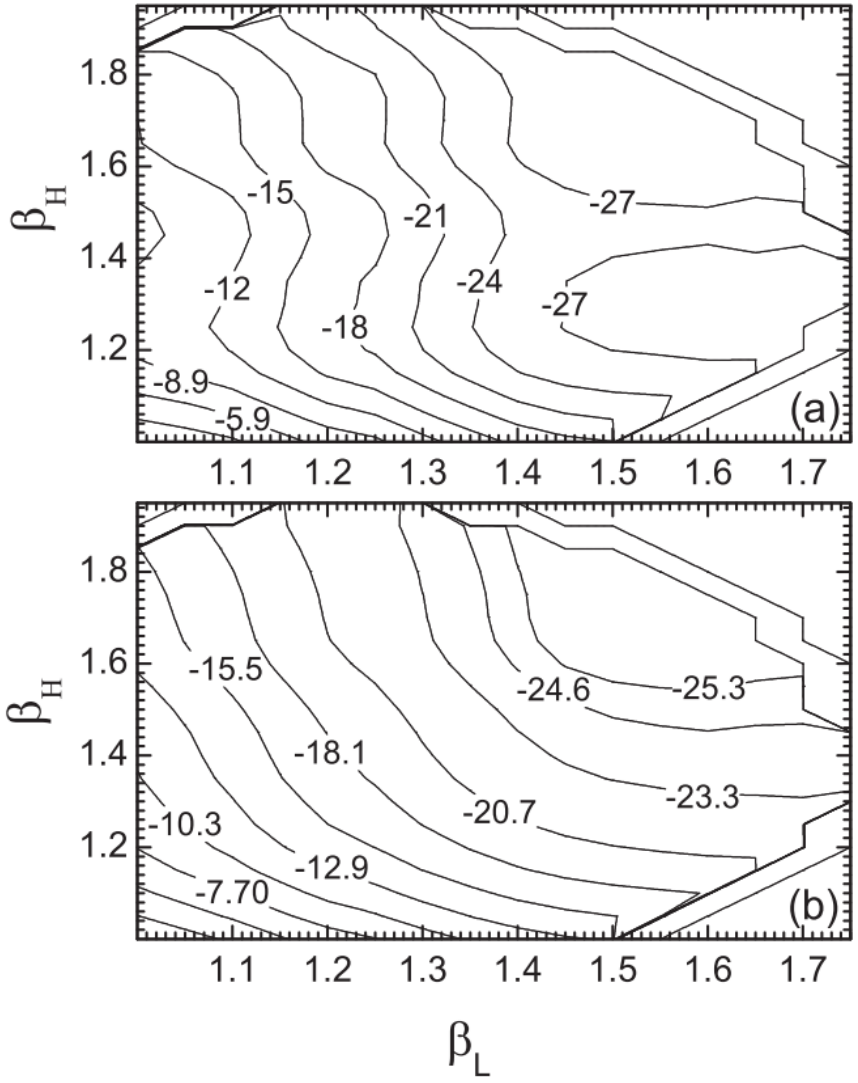

Energy surfaces for the DNS (A_1, Z_1)=(96, 36) and (A_2, Z_2)=(140, 56) for neutron energies E_n = 0 MeV (top) and E_n=55 MeV (bottom).

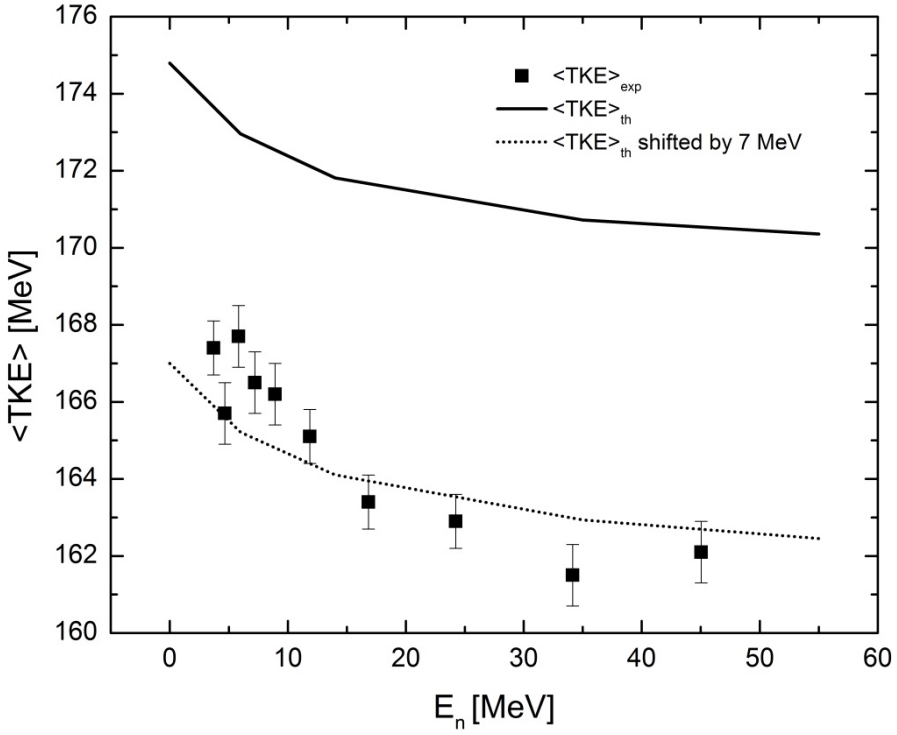

Average total kinetic energy as a function of neutron energy for ^{235}U (n,f) compared with experimental data. The configurations allowed are chosen such that the quasifission barrier is greater than 1 MeV.

Experimental data taken from:

- *R. Yanez et.al., Phys. Rev. C 89, 051604(R) (2014)*

Discussions – High excitation energy of the CN

$^{235}U(n,f)$

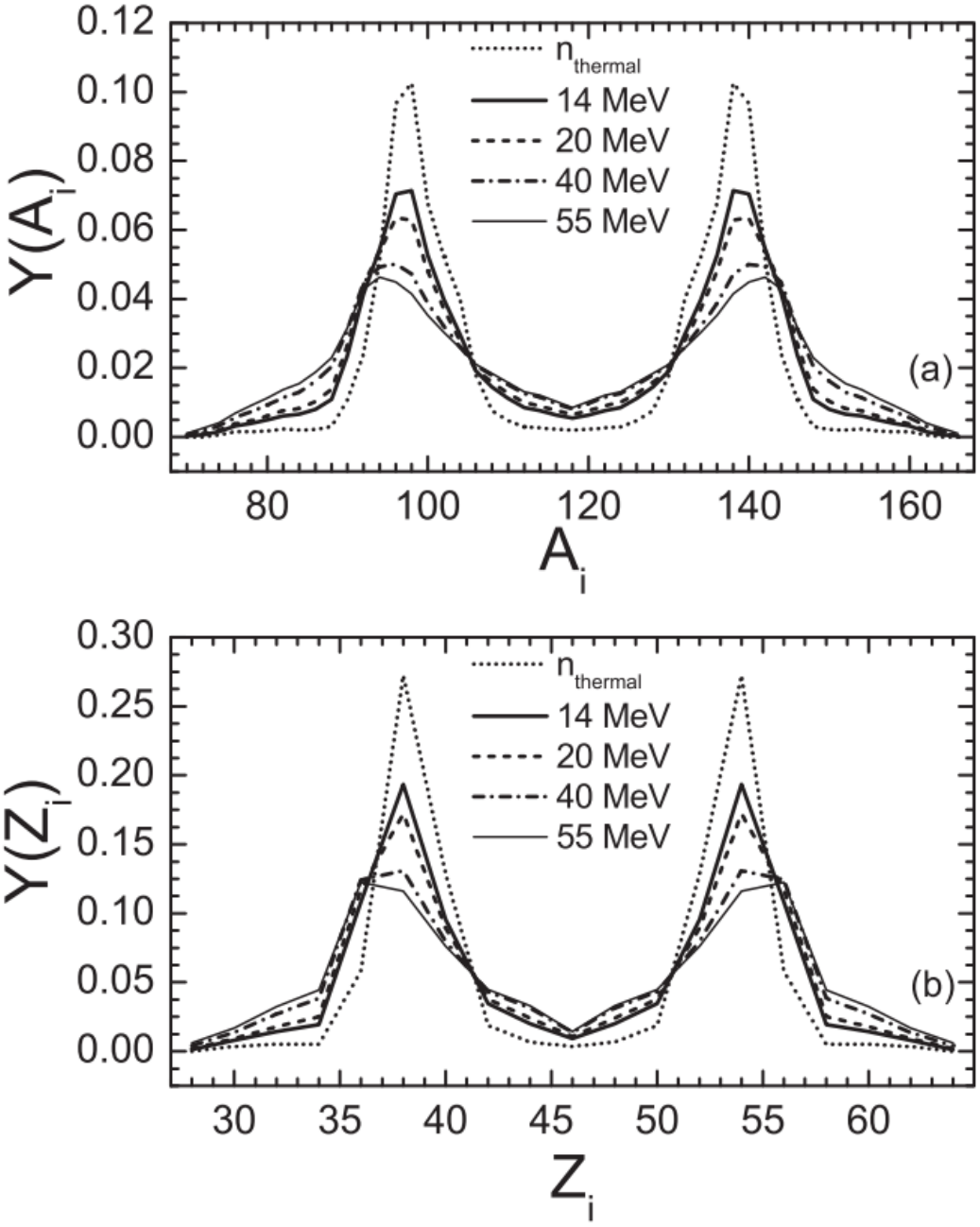

Discussions – High excitation energy of the CN

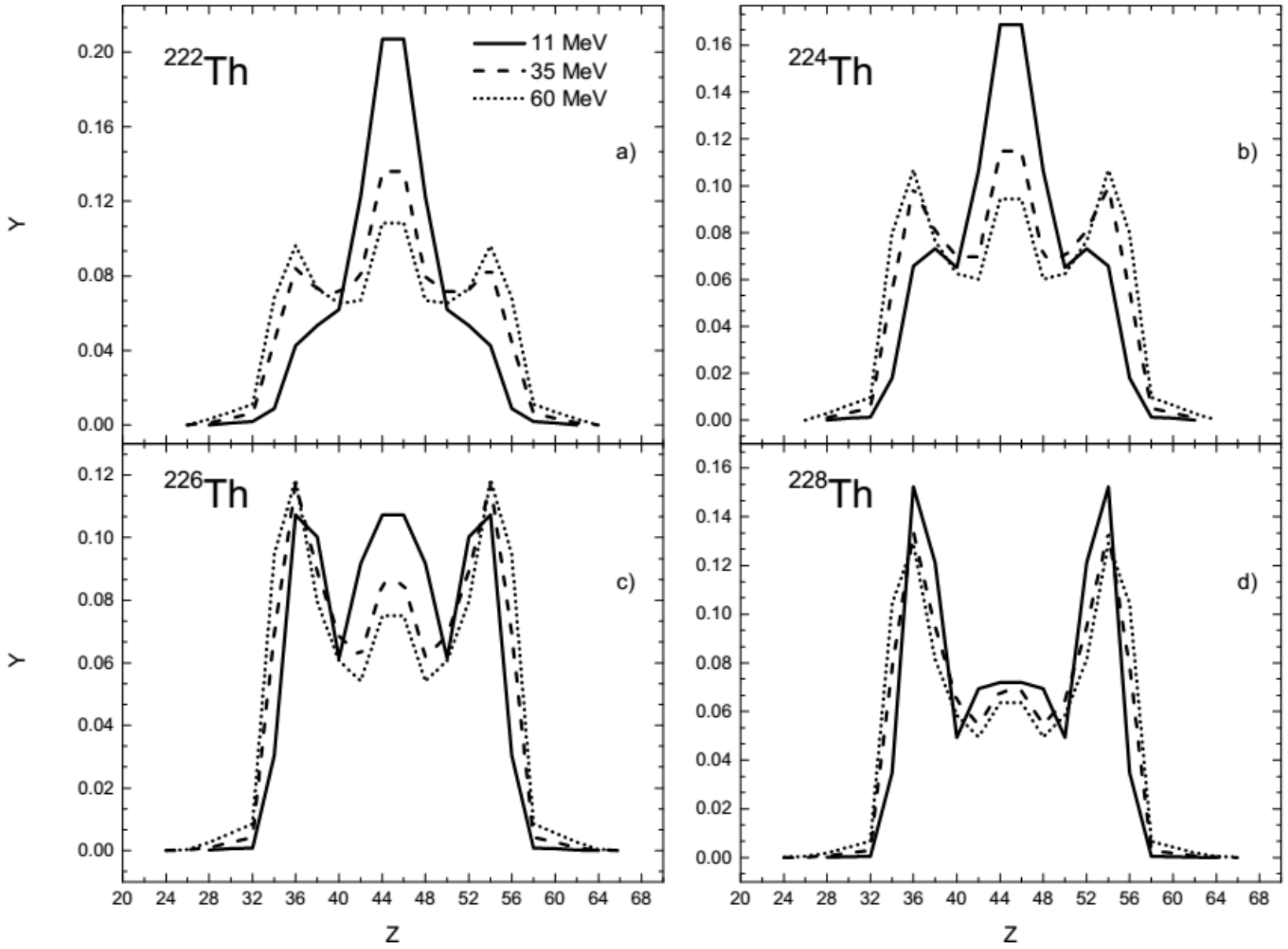

Predicted charge distributions for electromagnetic induced fission of Th isotopes at higher energies.

The angular momenta of fission fragments Collective spin component

- Two sources of angular momentum of fission fragments:
  - Orbital motion
  - Collective spin component (rotational-vibrational modes)

- These modes are:
  - a) Bending
  - b) Tilting
  - c) Twisting
  - d) Wriggling

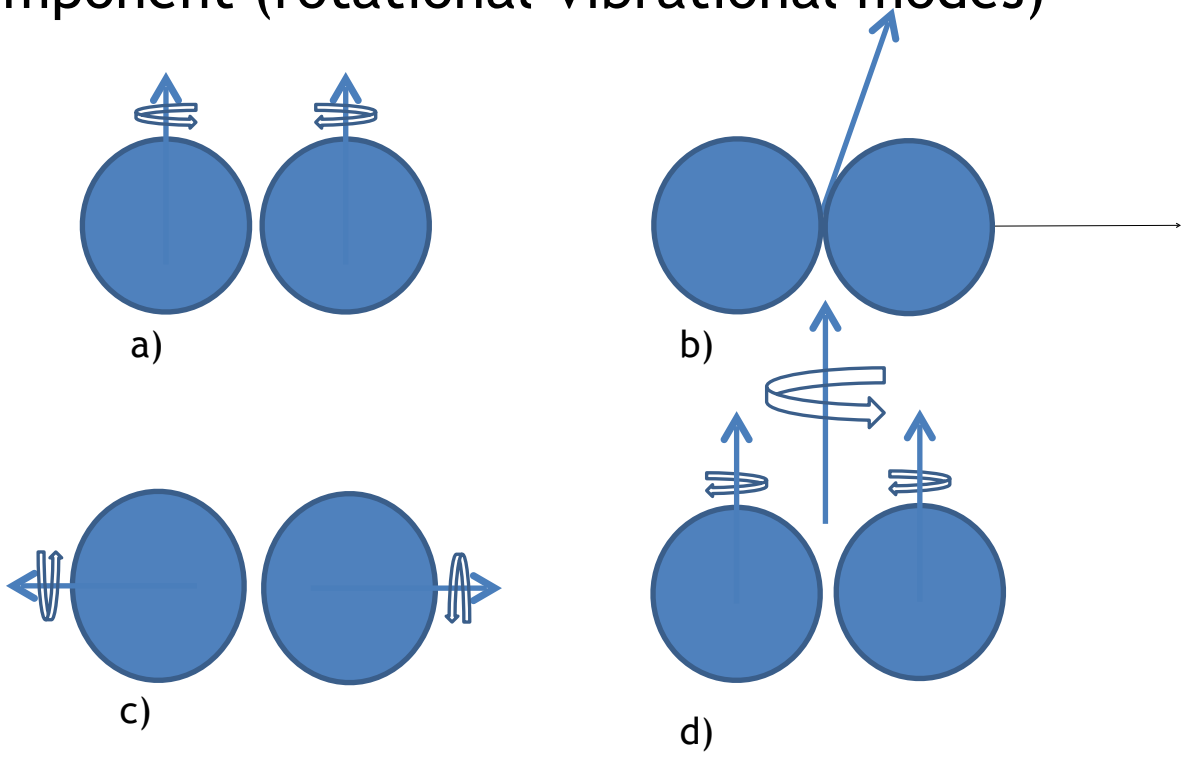

R.P.Schmitt, A.J.Pacheco, Nucl.Phys. A379, 313 (1982)

Fission fragment spins in thermal neutron induced fission of ^{252}Cf

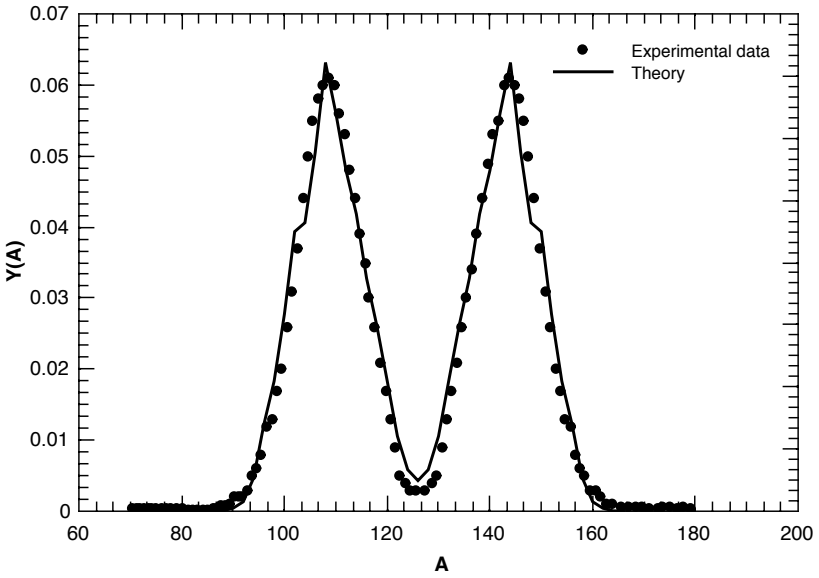

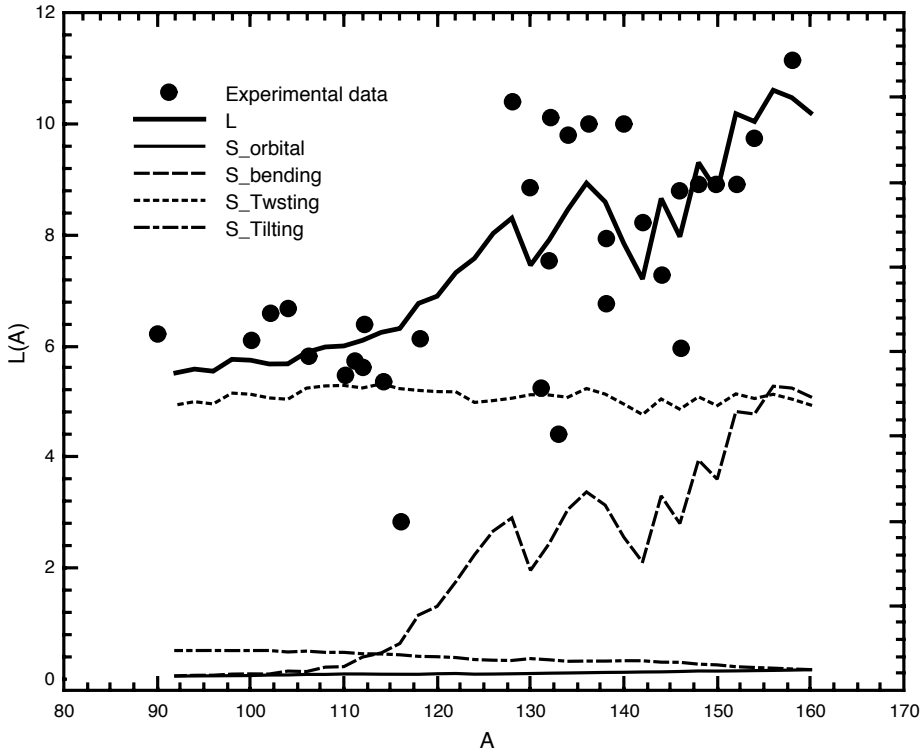

Experimental data taken from:
Romano et. al., PHYSICAL REVIEW C **81**, 014607 (2010)
Naik et.al., PHYSICAL REVIEW C **71**, 014304 (2005)

Results - the angular momentum of fission fragments

166 MeV $^{20}Ne+^{63}Cu$ [$E_{CN}^{*}(J = 0)=125$ MeV, $J_{max}=J_{cr}=51$]

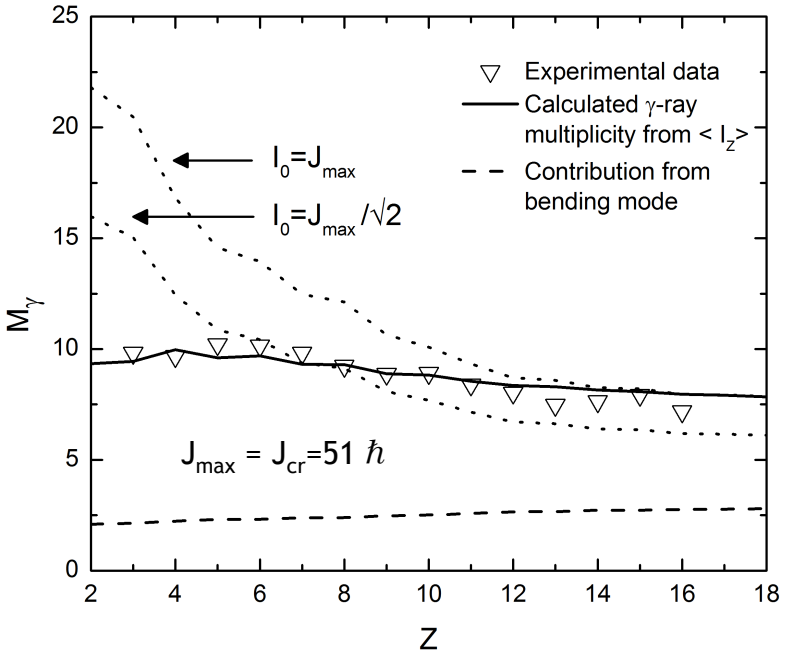

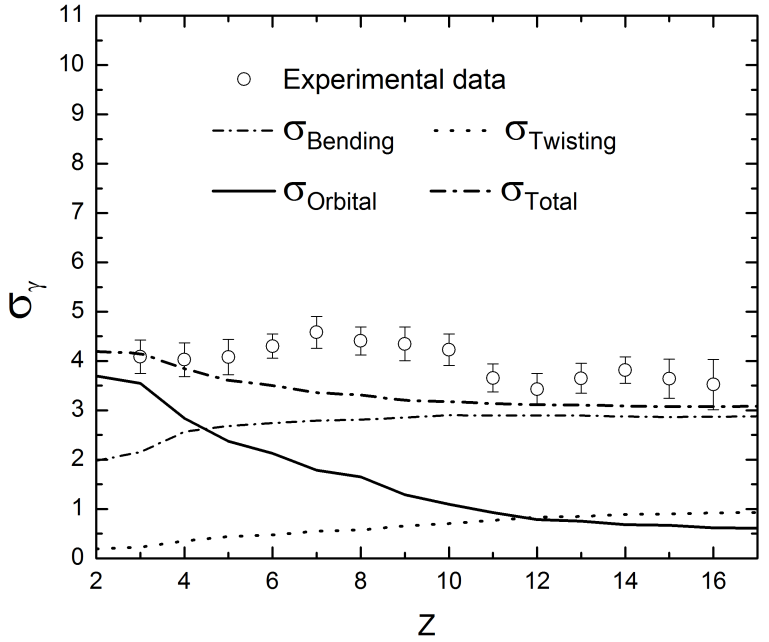

Angular momentum distribution of light systems shows a weak dependence with charge/mass.

The dispersion at lower masses (charges) is due to the orbital component, while at symmetry is given by the collective component.

H. Pașca, Sh. Kalandarov, G.G. Adamian, and N.V. Antonenko, *"Spins of complex fragments in binary reactions within dinuclear system model"*, sent to Phys. Rev. C.
Experimental data taken from R.A. Dayaras, et. al., Phys.Rev. C22, 1485 (1980)

Results - the angular momentum of fission fragments

175 MeV ^{20}Ne + ^{nat}Ag
[$E_{CN}^{*}(J = 0)$=128 MeV, J_{max}=J_{cr}=63]

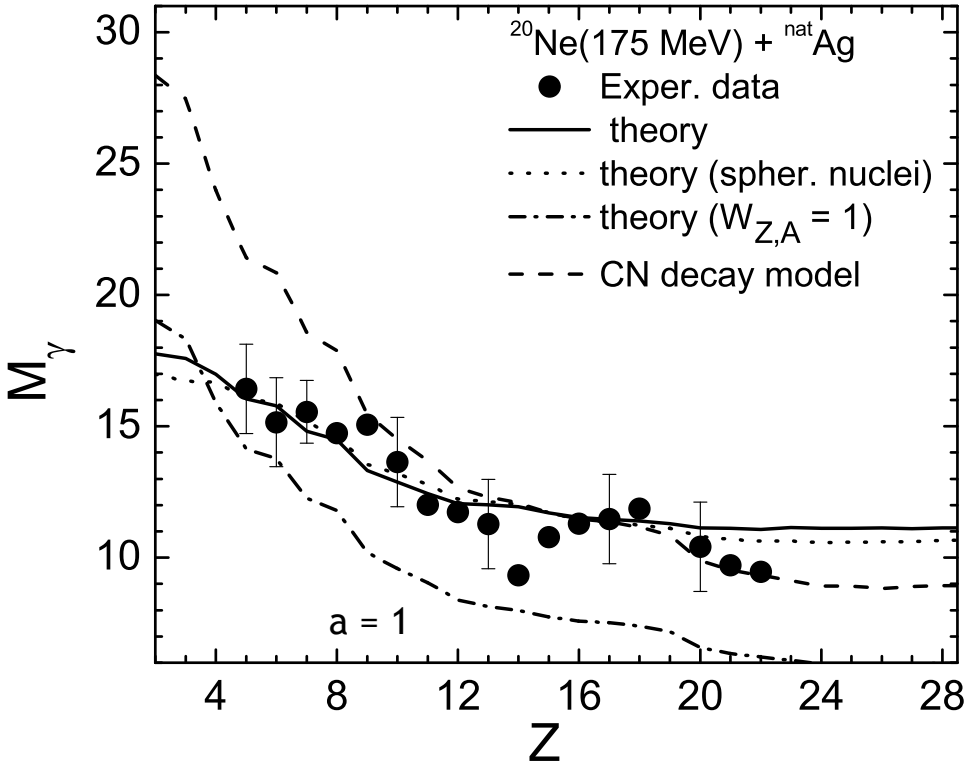

PHYSICAL REVIEW C VOLUME 21, NUMBER 1 JANUARY 1980

Equilibrium statistical treatment of angular momenta associated with collective modes in fission and heavy-ion reactions

Luciano G. Moretto and Richard P. Schmitt
Lawrence Berkeley Laboratory, University of California, Berkeley, California 94720
(Received 14 May 1979)

The first moment of the angular momentum is

$$\bar{l}(y) = l_{mx}\frac{[1-(T/\Re E_R^{mx})^{1/2}F((\Re E_R^{mx}/T)^{1/2})]\exp(\Re E_R^{mx}/T}{\exp(\Re E_R^{mx}/T)-1} \quad (1.7)$$

where

$$F(x) = e^{-x^2}\int_0^x e^{y^2}dy$$

H. Pașca, Sh. Kalandarov, G.G. Adamian, and N.V. Antonenko, *"Spins of complex fragments in binary reactions within dinuclear system model"*, sent to Phys. Rev. C.
Experimental data taken from L.G. Moretto, et.al.,Nucl.Phys. A502, 453c-472c (1989)

- *237 MeV $^{40}Ar+^{89}Y$*

[$E_{CN}^{*}(J = 0)=122$ MeV, $J_{max}=J_{cr}=78$]

Calculated γ-ray multiplicity (top) and average angular momentum of the heavy fragment (bottom) as a function of the charge number of the light fragment compared to experimental data.

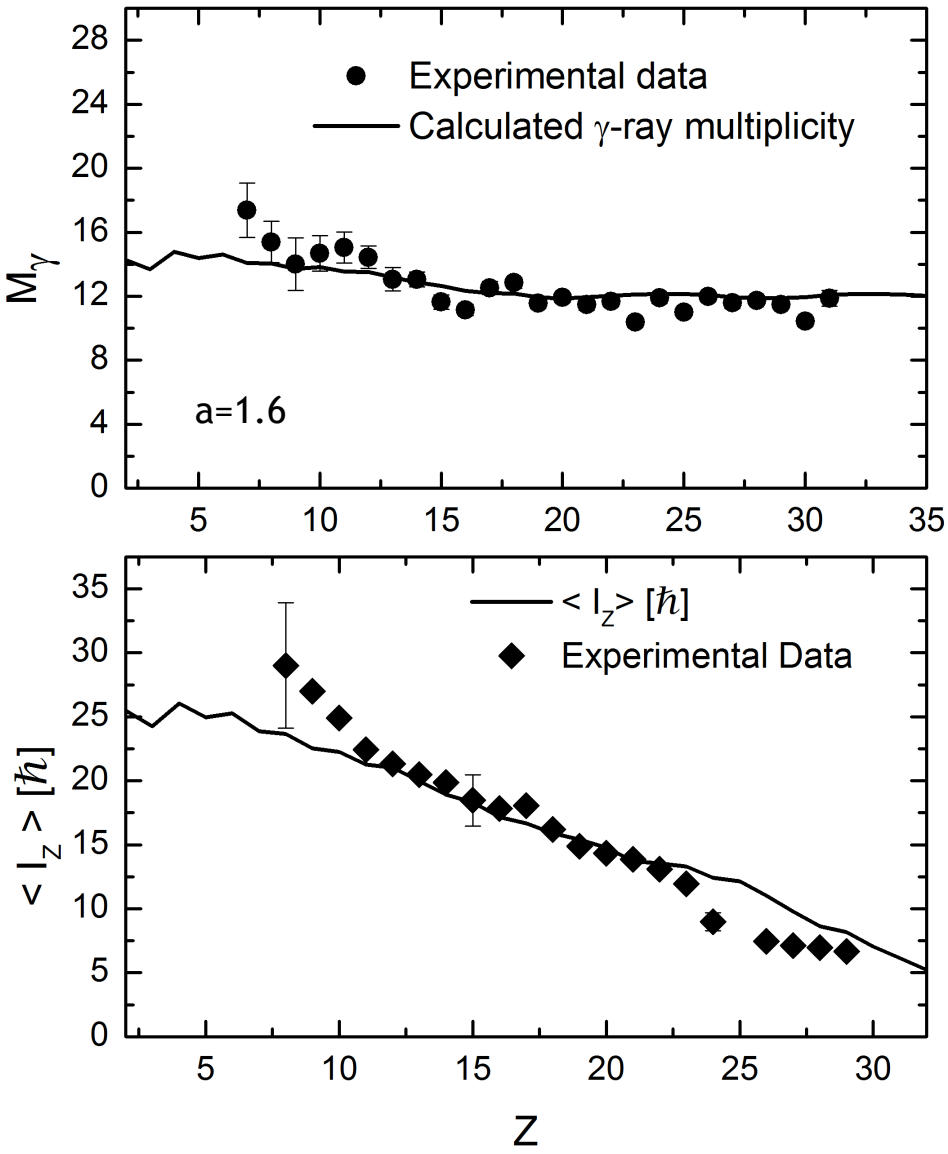

H. Pașca, Sh. Kalandarov, G.G. Adamian, and N.V. Antonenko, *"Spins of complex fragments in binary reactions within dinuclear system model"*, sent to Phys. Rev. C.
Experimental data taken from: up - L.G. Moretto, et.al.,Nucl.Phys. A502, 453c-472c (1989)
bottom - M.N.Namboodiri, et.al., Phys.Rev. C20, 982 (1979)

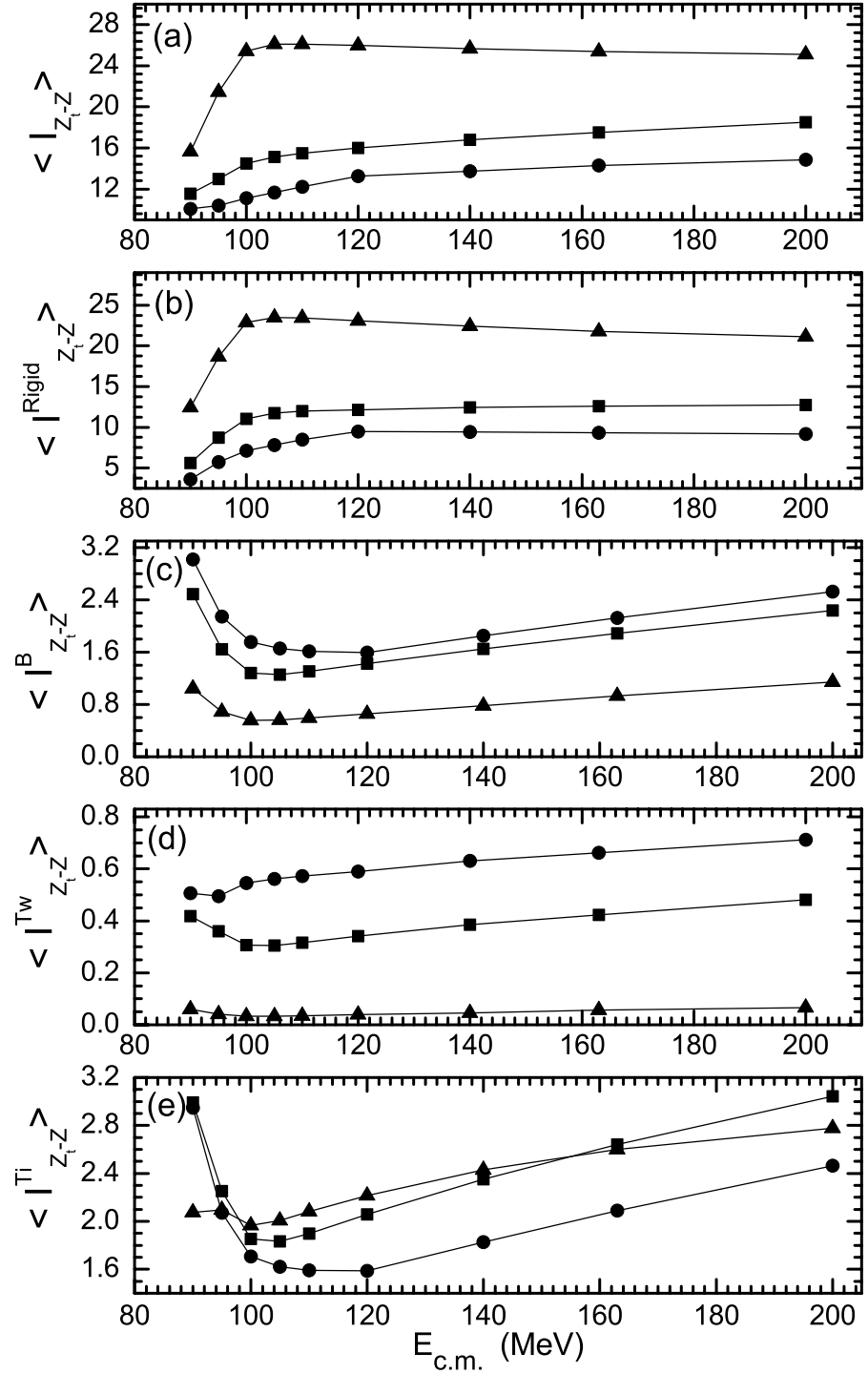

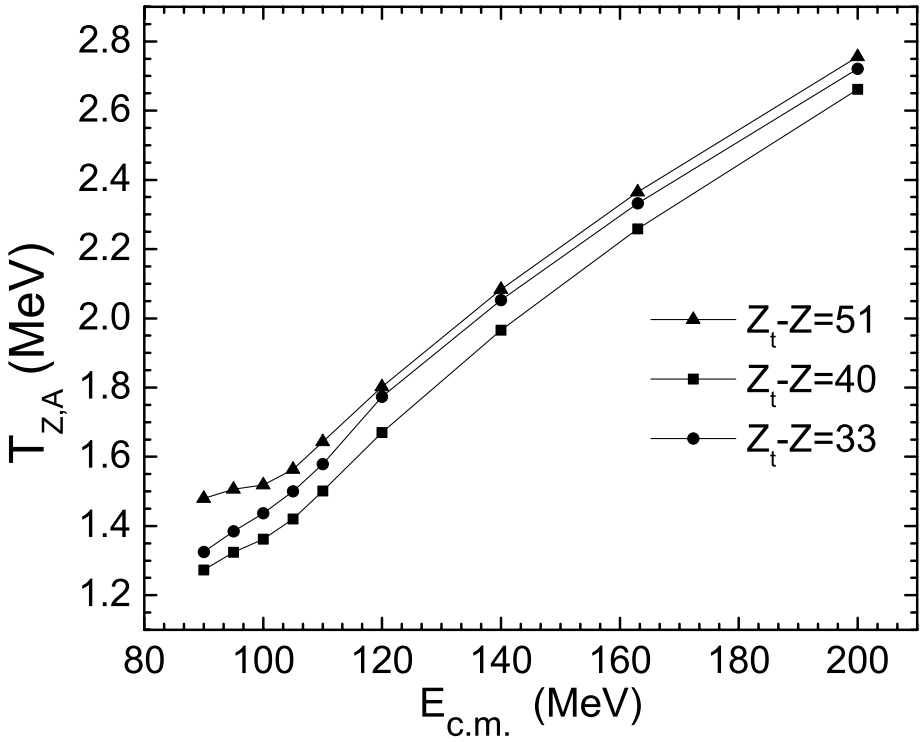

J_{cr}=78 $\hbar$.

H. Pașca, Sh. Kalandarov, G.G. Adamian, and N.V. Antonenko, *"Spins of complex fragments in binary reactions within dinuclear system model"*, sent to Phys. Rev. C.

Results - the angular momentum of fission fragments

Role of the entrance channel

Saturation of angular momentum after J_{cr} is reached.

$^{40}Ar+^{107,109}$ Ag reaction at 288 MeV and 340 MeV (a=5, $E_{CN}^{*}(J = 0)$=236,288 MeV, respectively, $J_{max}=J_{cr}$=97).

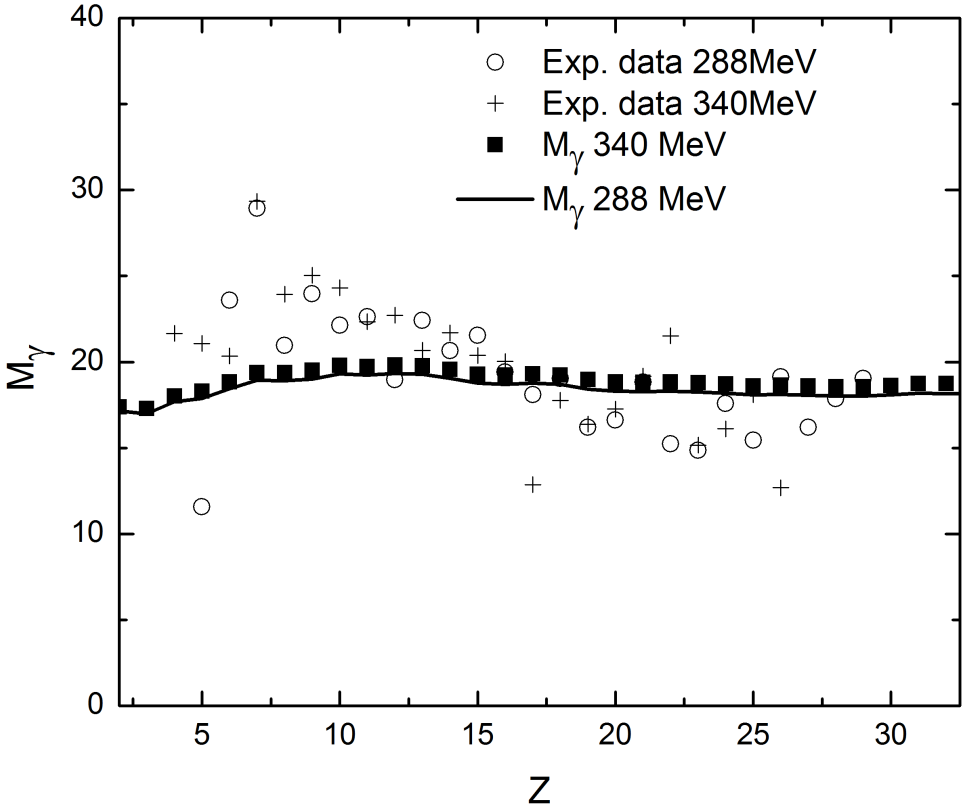

H. Pașca, Sh. Kalandarov, G.G. Adamian, and N.V. Antonenko, *"Spins of complex fragments in binary reactions within dinuclear system model"*, sent to Phys. Rev. C.
Experimental data taken from L.G. Moretto, LBL-9130; CONF-790751-1; CONF-790751-2

Spin distribution structure of heavier systems

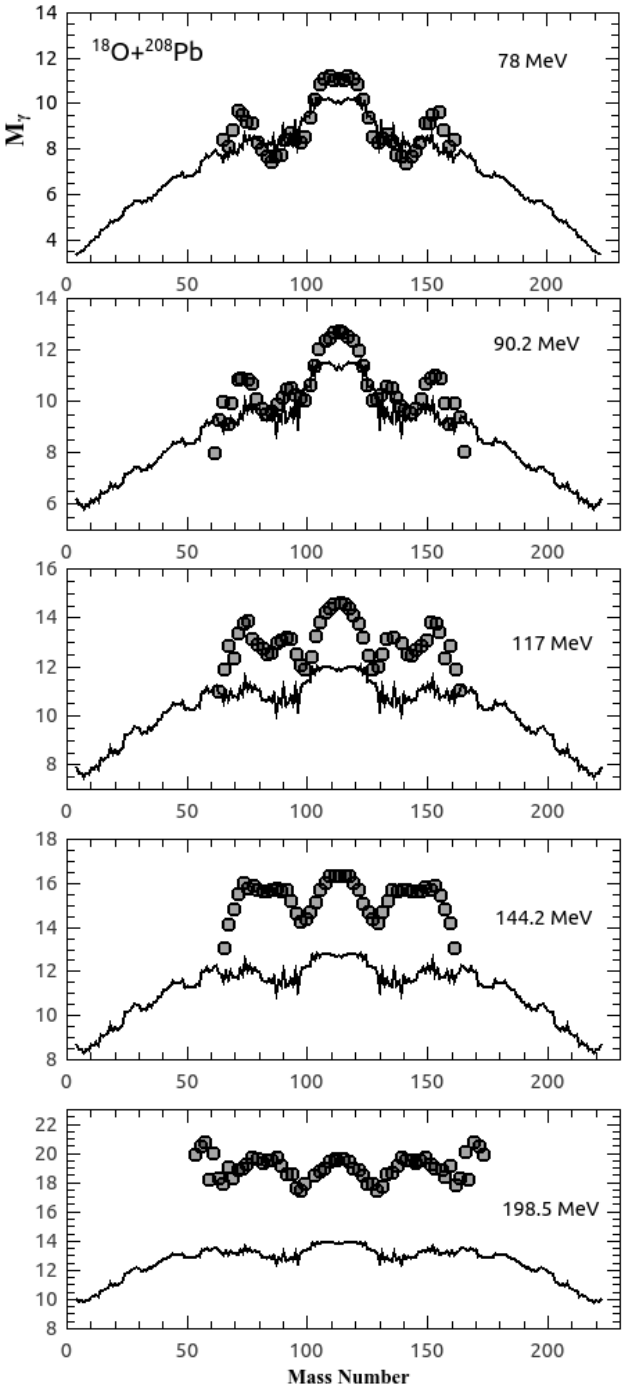

E*=11 MeV

$^{18}O+^{208}Pb->226Th^*$

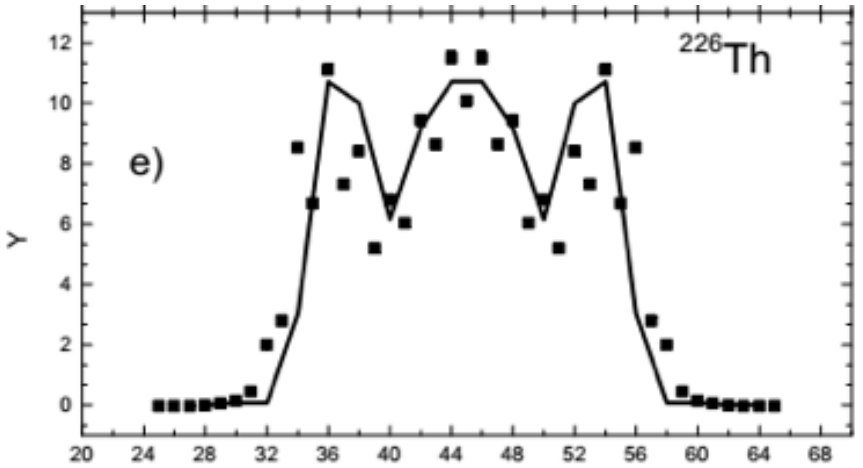

$^{18}O+^{208}Pb->226Th^*$ (90 MeV)

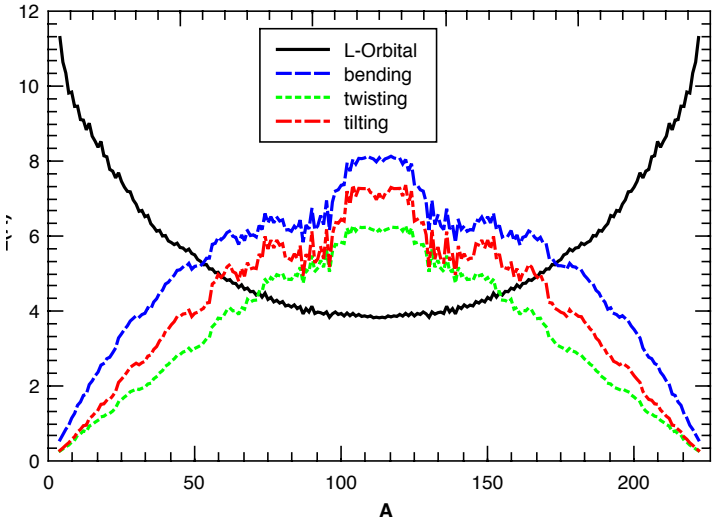

E_{Lab}	$E_{CN}^*(J=0)$	L_{max}
78	26 MeV	3
90	37 MeV	25
117	62 MeV	61
144	86 MeV	73
190	136 MeV	73

$$I = 2(M_\gamma - a) \quad , a = 0...6$$

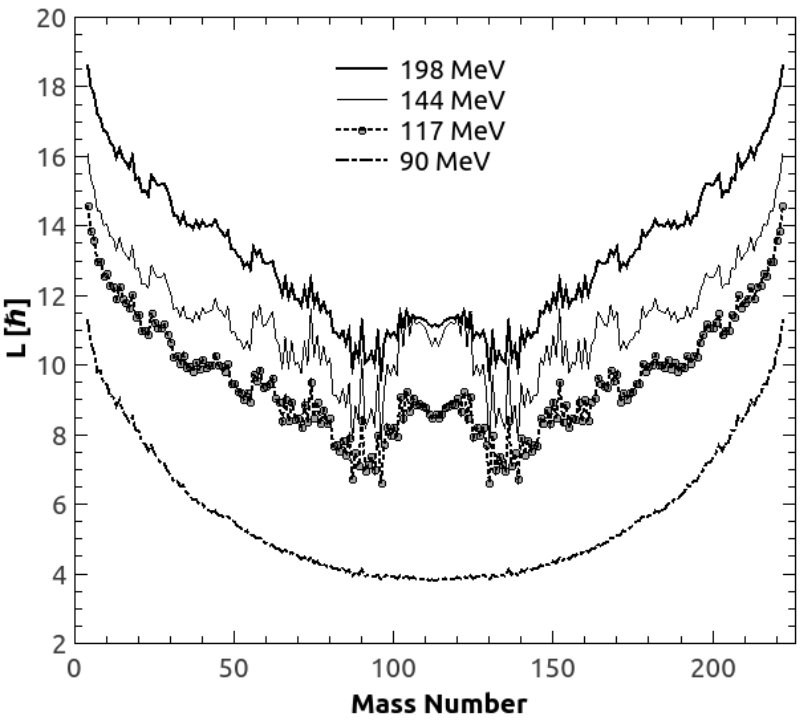

$^{18}O+^{208}Pb->226Th^{*}$

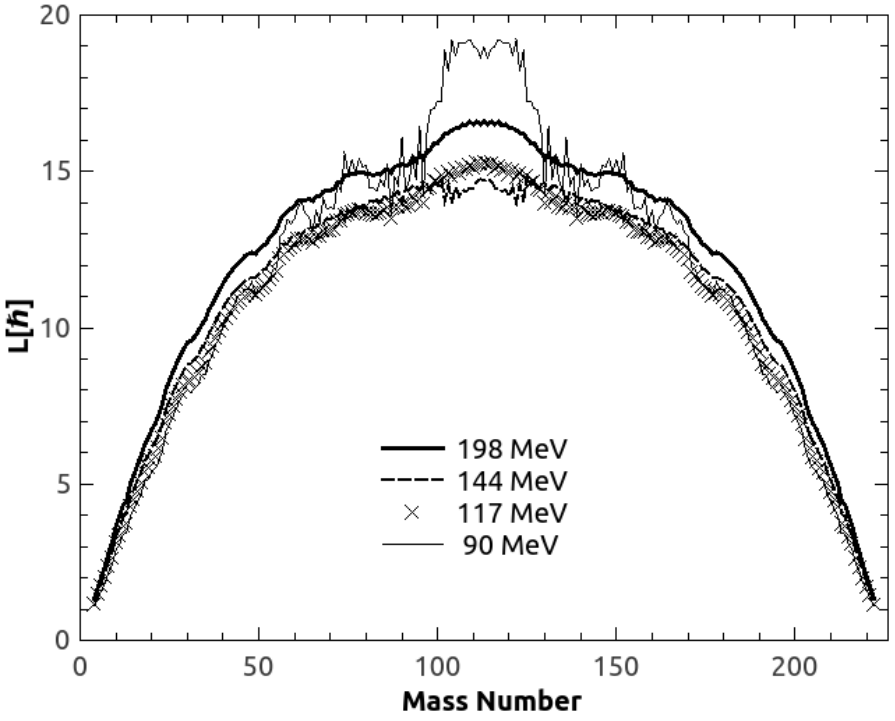

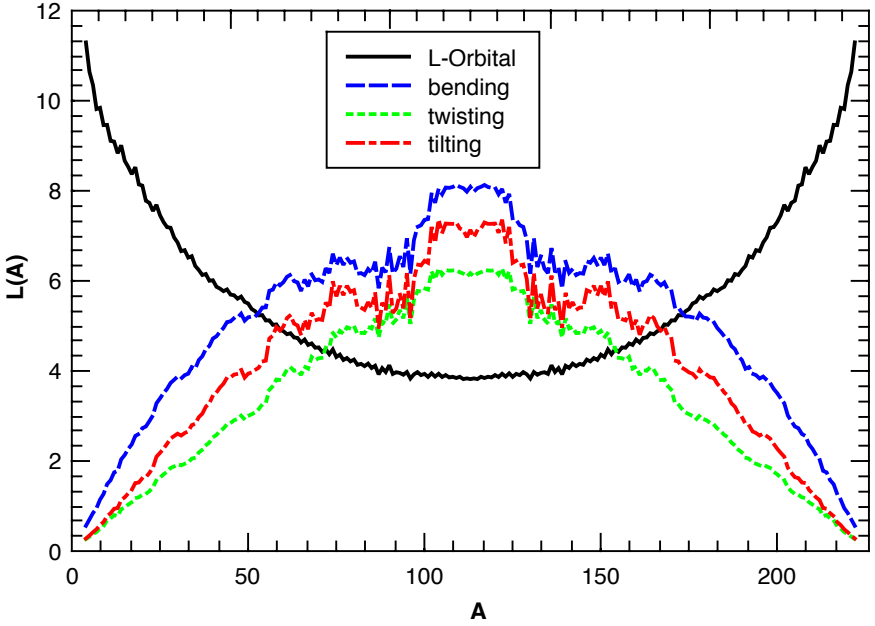

- The bending, tilting and twisting modes are the major source of angular momentum of the fission fragments at low bombarding energies; the potential energy surface influences the temperature of the decaying DNS, and therefore the collective spin distribution exhibits a structure in mass/charge coordinate correlated with the driving potential.

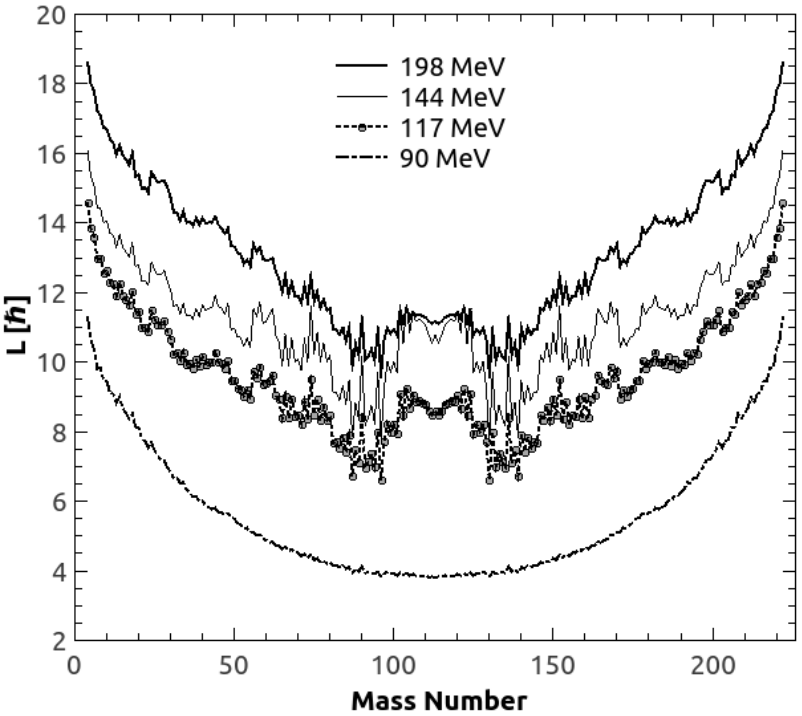

$^{18}O+^{208}Pb->226Th^{*}$

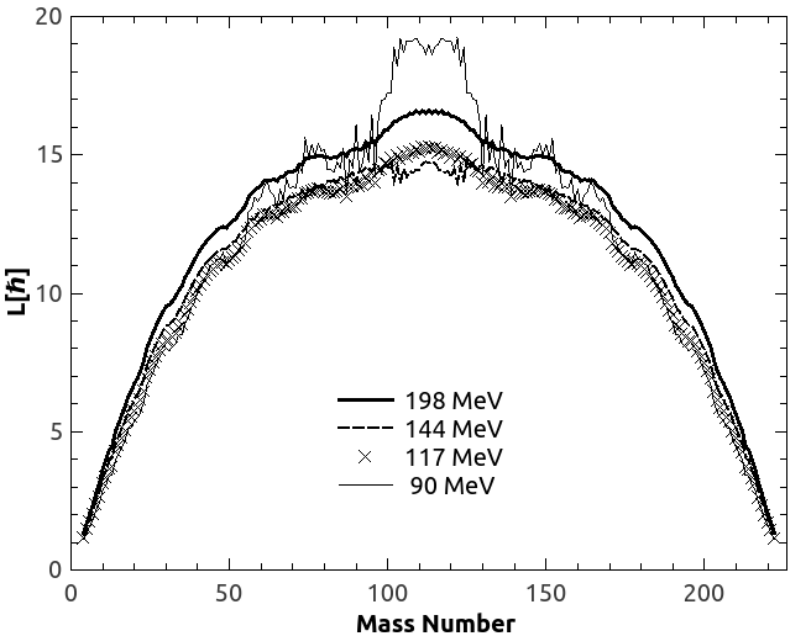

- For high bombarding energies
  - the rigid rotation component of the spin distribution increases and starts to exhibit maxima at mass/ charge coordinates where the driving potential presents minima.
  - the structure of the collective component distribution gets smoother, due to the increase of the average angular momentum of the DNS which hinders the enhancement of the spin due to temperature.

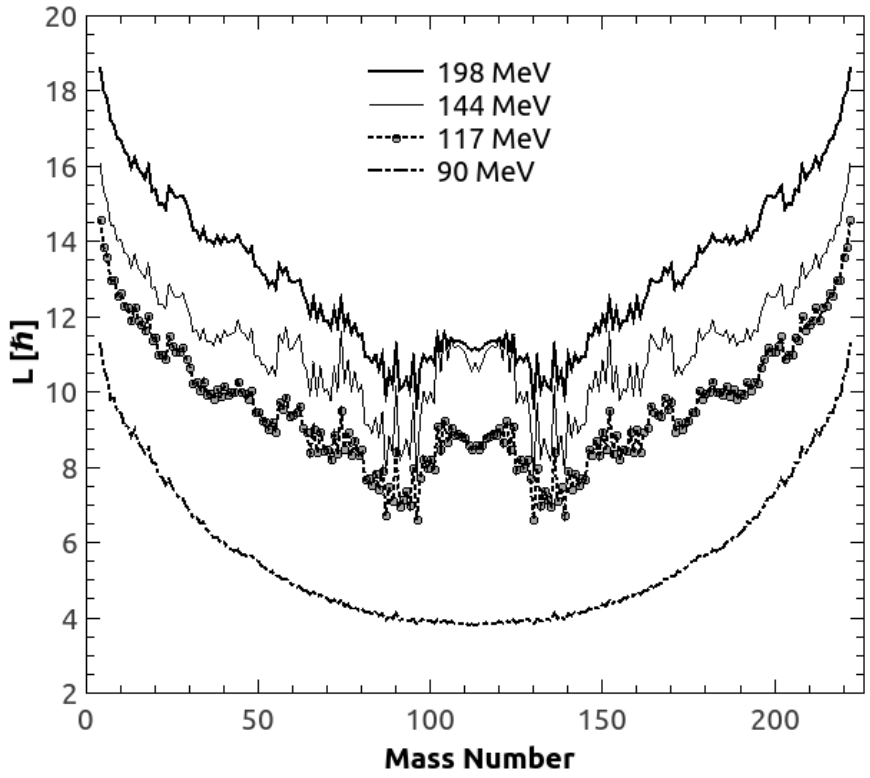

$^{18}O+^{208}Pb->226Th^{*}$

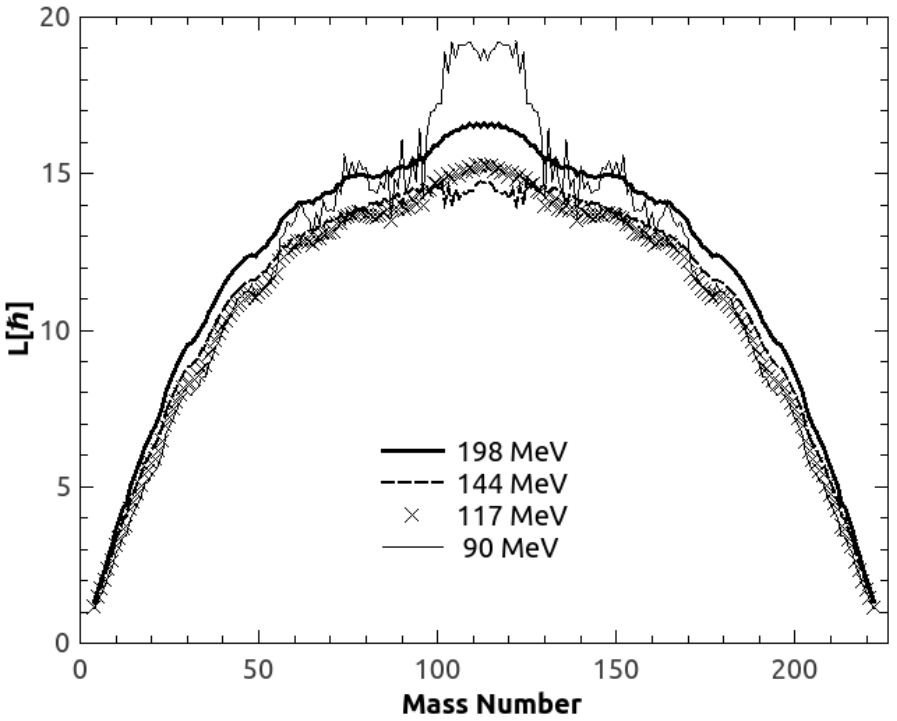

At even higher bombarding energies

- The high excitation energy makes the previously energetically unfavorable configurations more likely to occur, which smooths out the distribution due to orbital motion -> angular momentum of the asymmetric fragments increase towards the saturation limit.
- Collective spin component increases due to high temperature.

Conclusions

- The charge and mass yields at various excitation energies are shown to be the result of the interplay between the macroscopic and microscopic energies.
- At high excitation energies we predict the *conservation of the asymmetry of the charge/ mass yields in the $^{235}U(n,f)$ reaction*, as well as l*arge asymmetric fission modes in the high excitation energy of Th isotopes*.
- The *angular momenta of the fission fragments is* demonstrated to be *intimately related to* the charge/mass yields, and, consequently, *to the entrance channel*.
- The structure of the spin distribution is related to the interplay between the orbital and the collective components.
- We predict the s*aturation of the orbital component* of the spin distribution *at large bombarding energies*.
- *In the case of the spontaneous fission of ^{252}Cf, the bending and twisting modes are the main source of angular momentum of the fission fragments*.
- In the case of heavy-ion reactions, *at large mass/charge asymmetry, the orbital motion is the main component of the angular momentum* for all energies in question. For low bombarding energies (low angular momentum of the CN), *at symmetry, the spin collective modes* are the main source of FF angular momenta, while at high projectile energies the two components bear equal weight.

Thank you!

$$< I_{Z,A} >= \frac{\sum_{J=0}^{J_{max}} I^{T}_{Z,A}(J)\sigma_{Z,A}(E_{c.m.},J)}{\sum_{J=0}^{J_{max}} \sigma_{Z,A}(E_{c.m.},J)}$$

$$\begin{aligned} I^{T}_{Z,A}(J) &= I^{Rigid}_{Z,A}(J) + I^{Bearing}_{Z,A}(J) \\ &= I^{Rigid}_{Z,A}(J) + I^{Tw}_{Z,A}(J) + I^{Ti}_{Z,A}(J) + I^{B}_{Z,A}(J) \end{aligned}$$

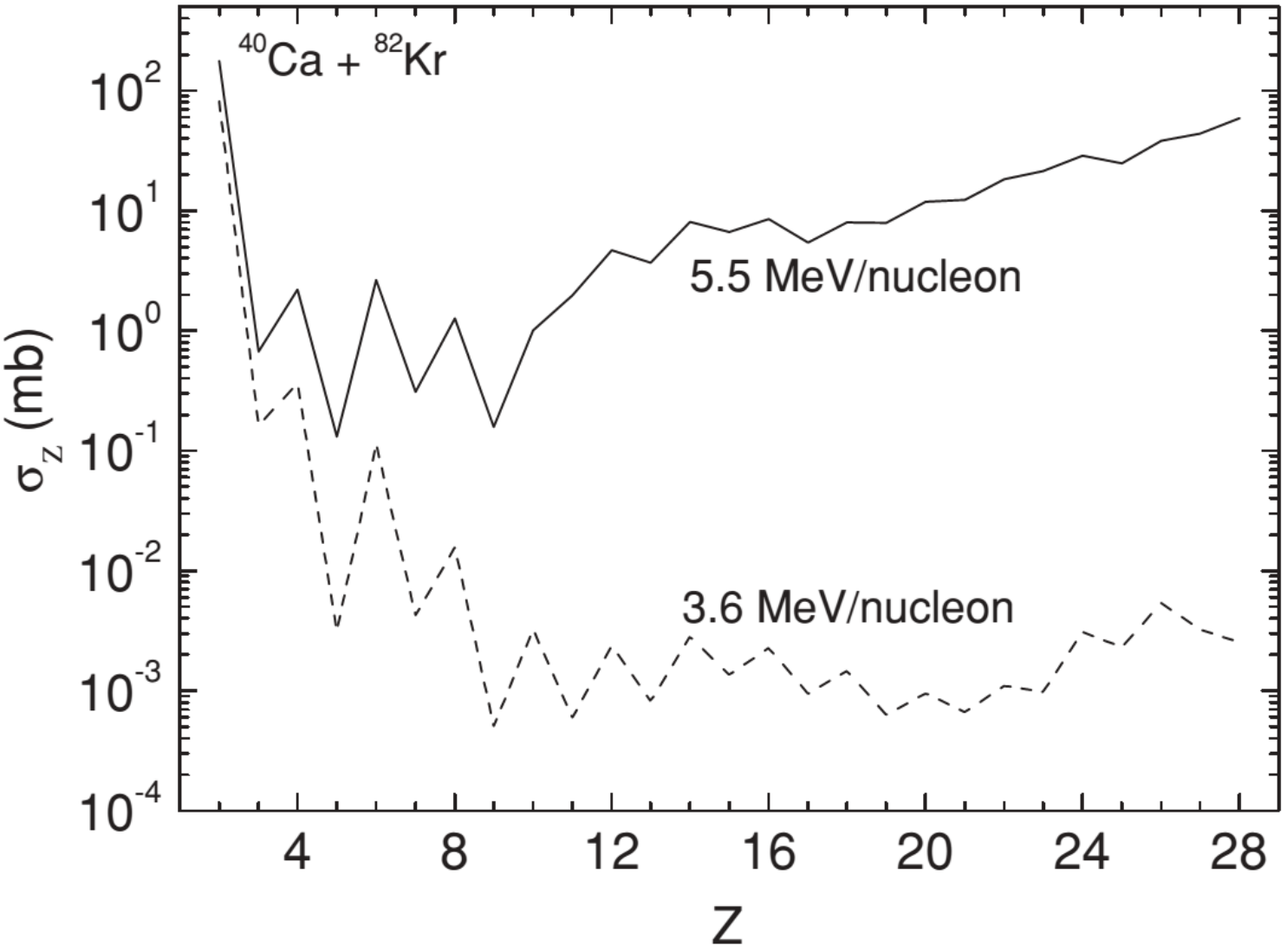
^{40}Ca + ^{82}Kr
5.5 MeV/nucleon
3.6 MeV/nucleon
σ_Z (mb)
Z
10^{2}
10^{1}
10^{0}
10^{-1}
10^{-2}
10^{-3}
10^{-4}
4
8
12
16
20
24
28

Role of entrance channel

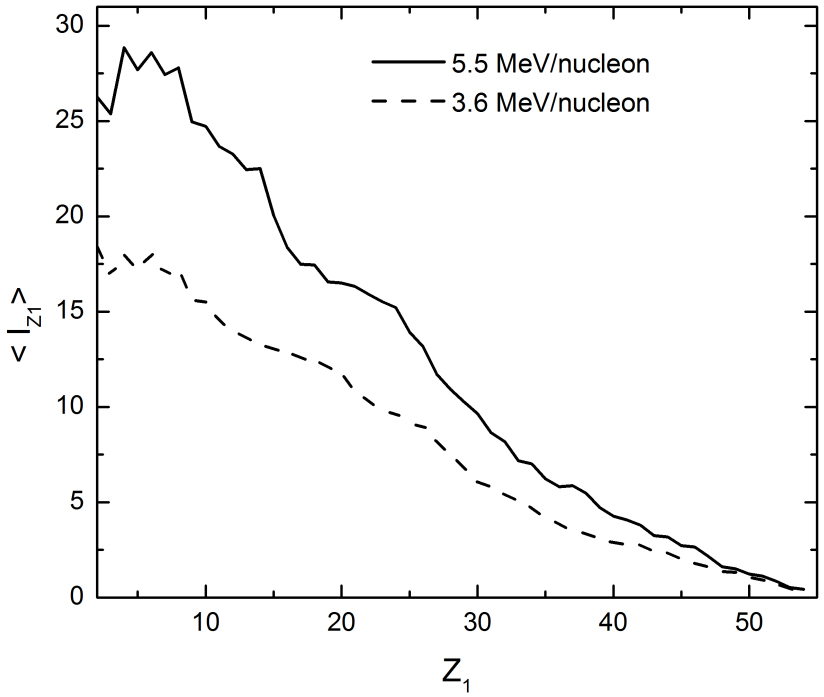

$^{40}Ca+^{82}Kr$

$3.6MeV \rightarrow J_{max} = J_{kin} = 32\hbar$

$5.5MeV \rightarrow J_{max} = J_{cr} = 75\hbar$

Both reactions lead to the formation of the same CN ^{122}Ba with the excitation energies $E^*_{3.6MeV}(J = 0) = 55MeV$ and $E^*_{5.5MeV}(J = 0) = 105$ MeV.

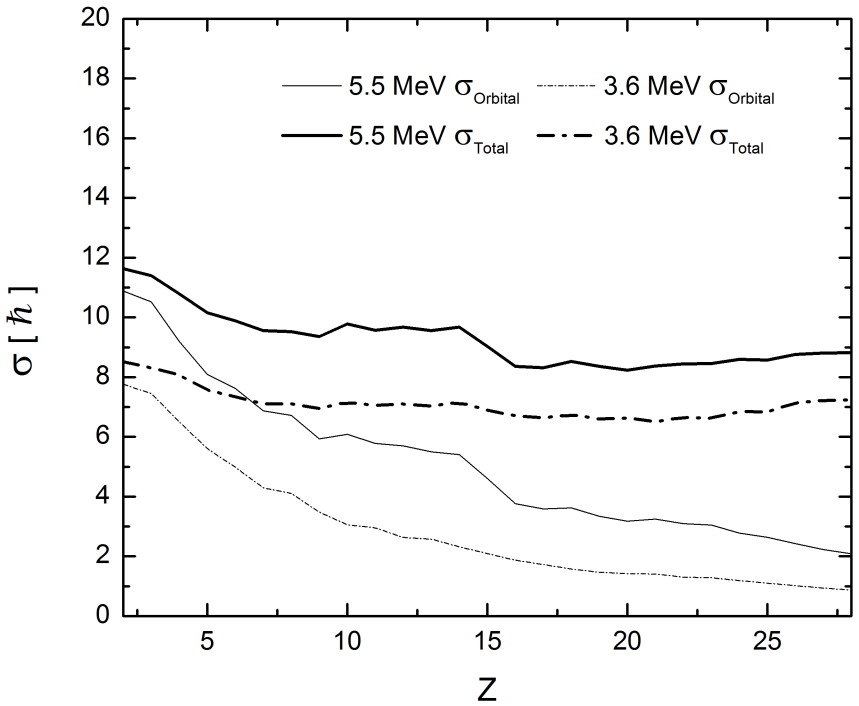

The 5.5MeV reaction will impart greater angular momentum to the fission fragments because of the higher value of the orbital angular momentum injected into the system.

H. Pașca, Sh. Kalandarov, G.G. Adamian, and N.V. Antonenko, *"Spins of complex fragments in binary reactions within dinuclear system model"*, sent to Phys. Rev. C.

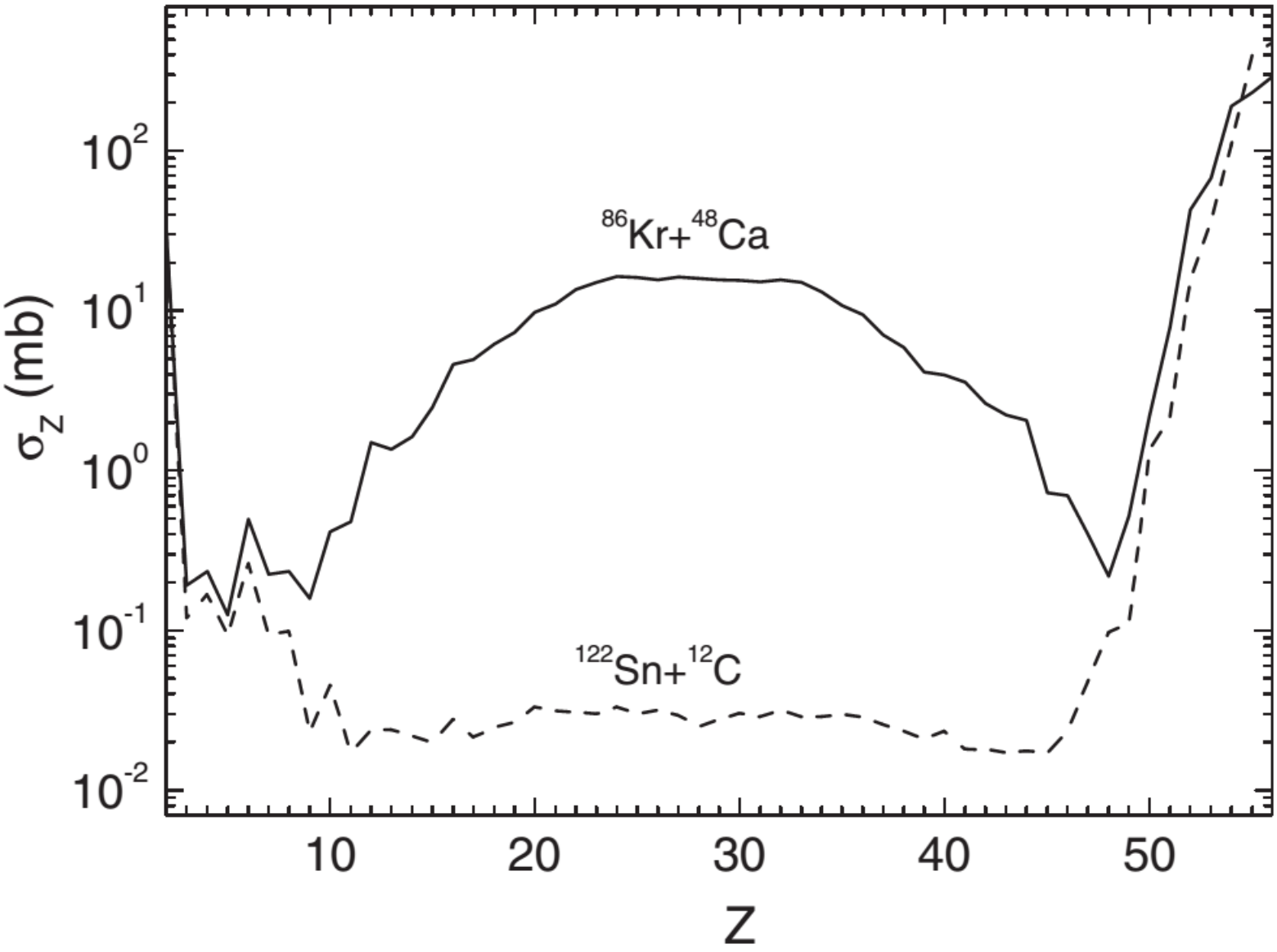
10^2
10^1
10^0
10^{-1}
10^{-2}
σ_Z (mb)
^{86}Kr+^{48}Ca
^{122}Sn+^{12}C
10
20
30
40
50
Z

Role of entrance channel

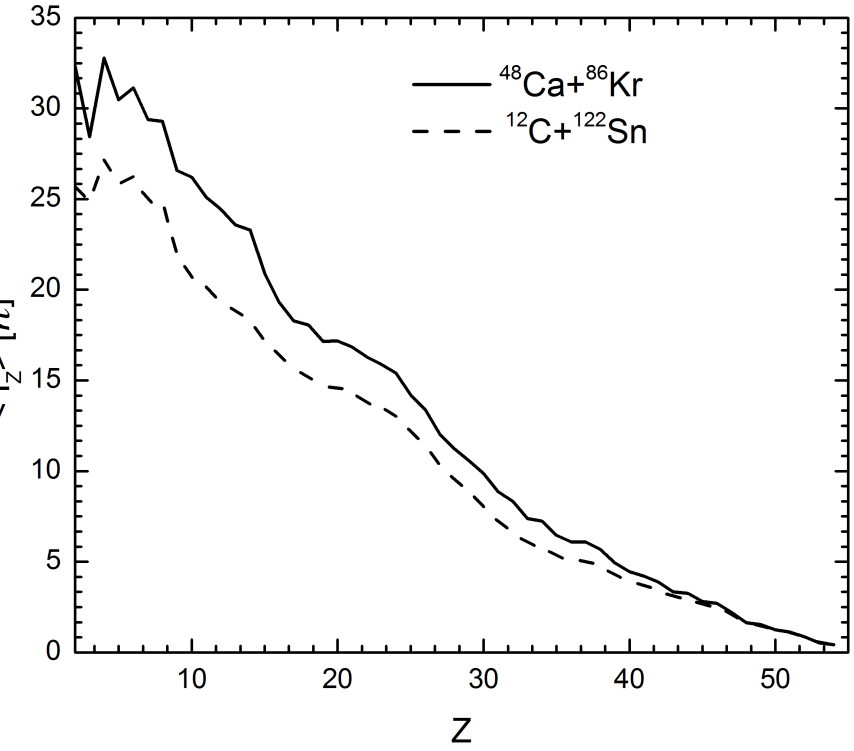

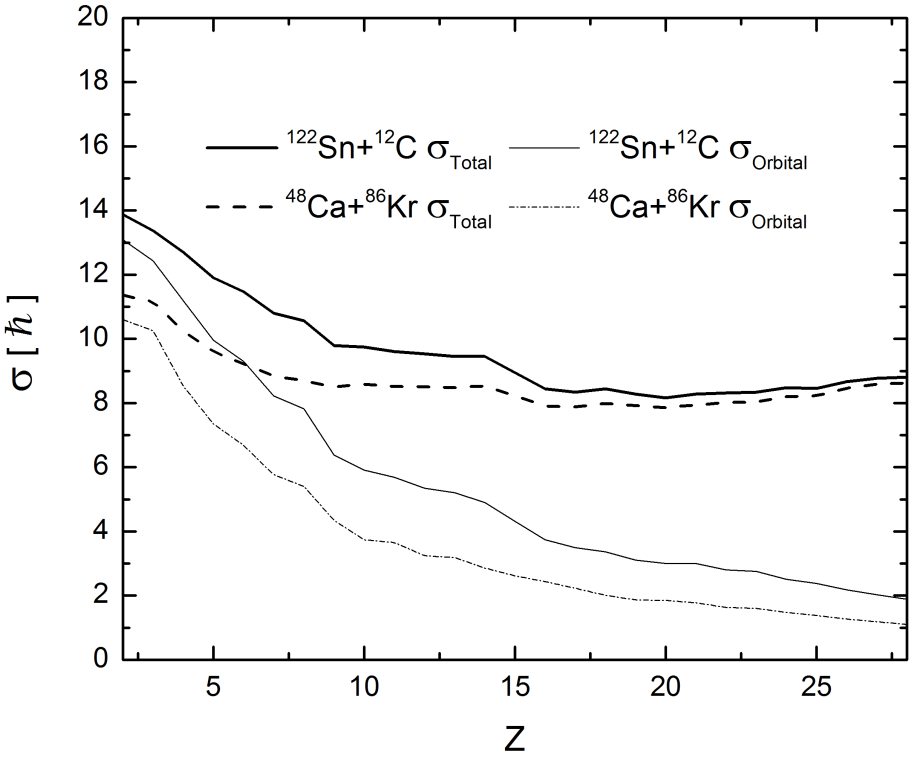

$^{48}Ca+^{86}Kr$(5.5 MeV/nucleon, J_{max} = 88) and$^{12}C+^{122}Sn$ (12MeV/nucleon, Jmax = 47) lead to lead to the same CN, ^{134}Ba , with the same excitation energy E∗CN(J =0) = 130 MeV.

H. Pașca, Sh. Kalandarov, G.G. Adamian, and N.V. Antonenko, *"Spins of complex fragments in binary reactions within dinuclear system model"*, sent to Phys. Rev. C.

Discussions – High excitation energy of the CN

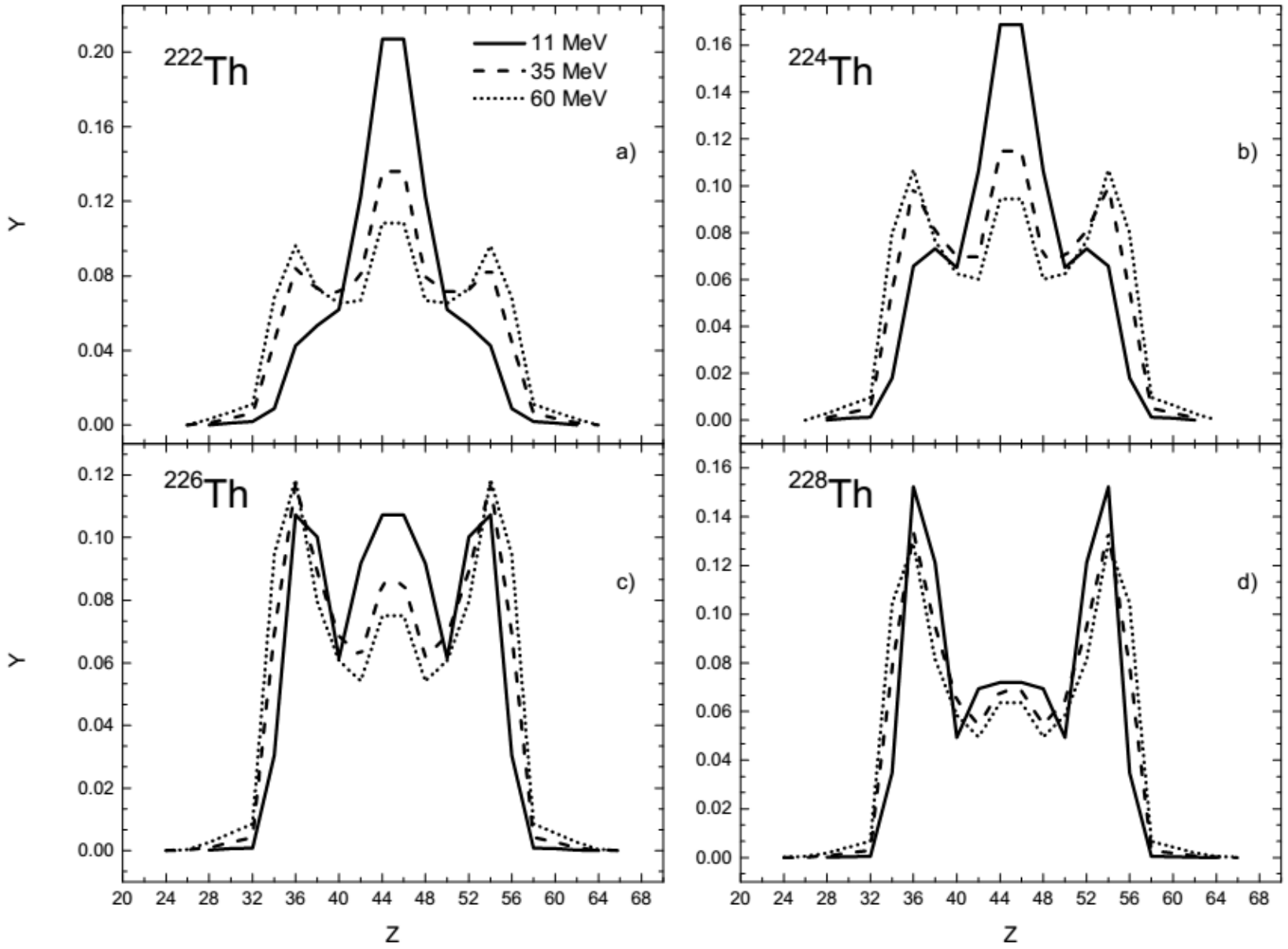

Predicted charge distributions for electromagnetic induced fission of Th isotopes at higher energies.

Discussions – High excitation energy of the CN

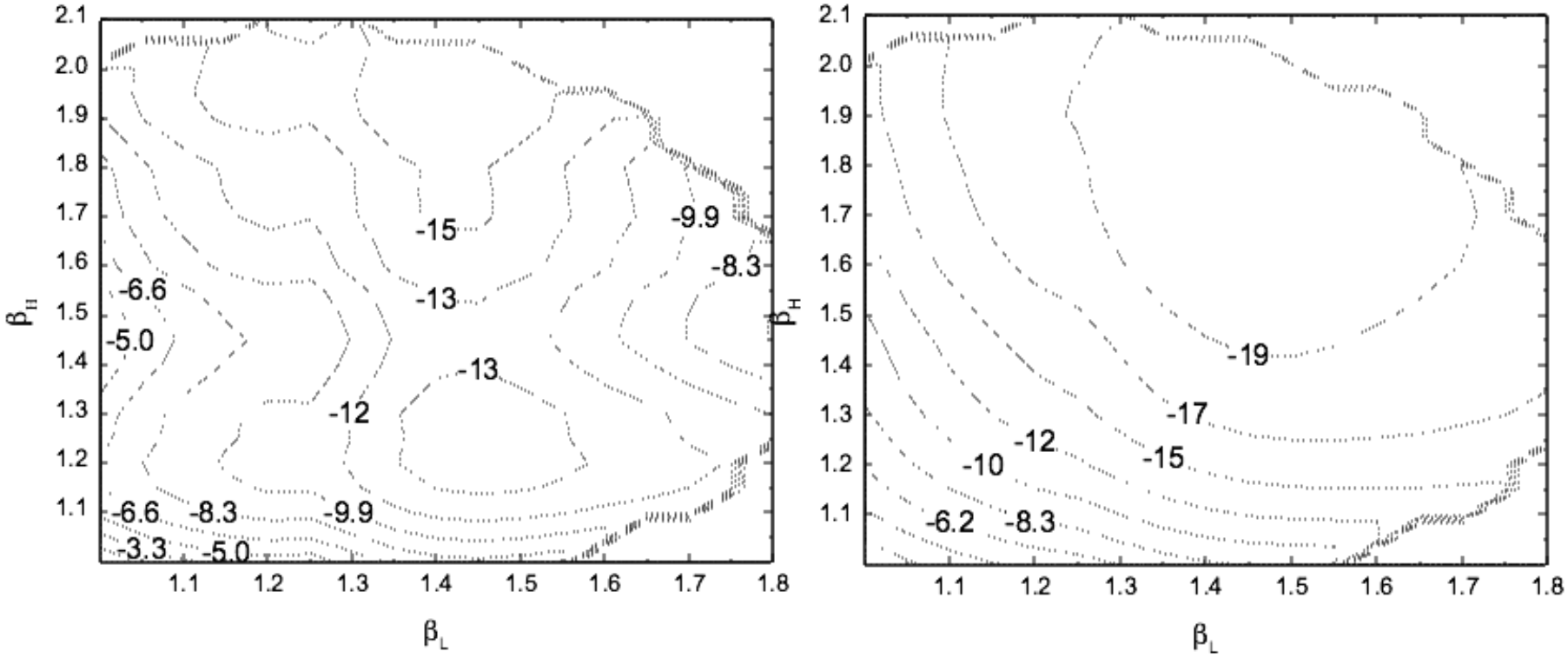

^{86}Kr + ^{136}Xe energy surfaces for E^*_{CN} = 11 (Left) and E^*_{CN} = 60 MeV (Right)

$$Y(A_i, Z_i) = N_0 \int\int W(A_i, Z_i, \beta_1, \beta_2, E^*)\, \mathrm{d}\beta_1 \mathrm{d}\beta_2$$

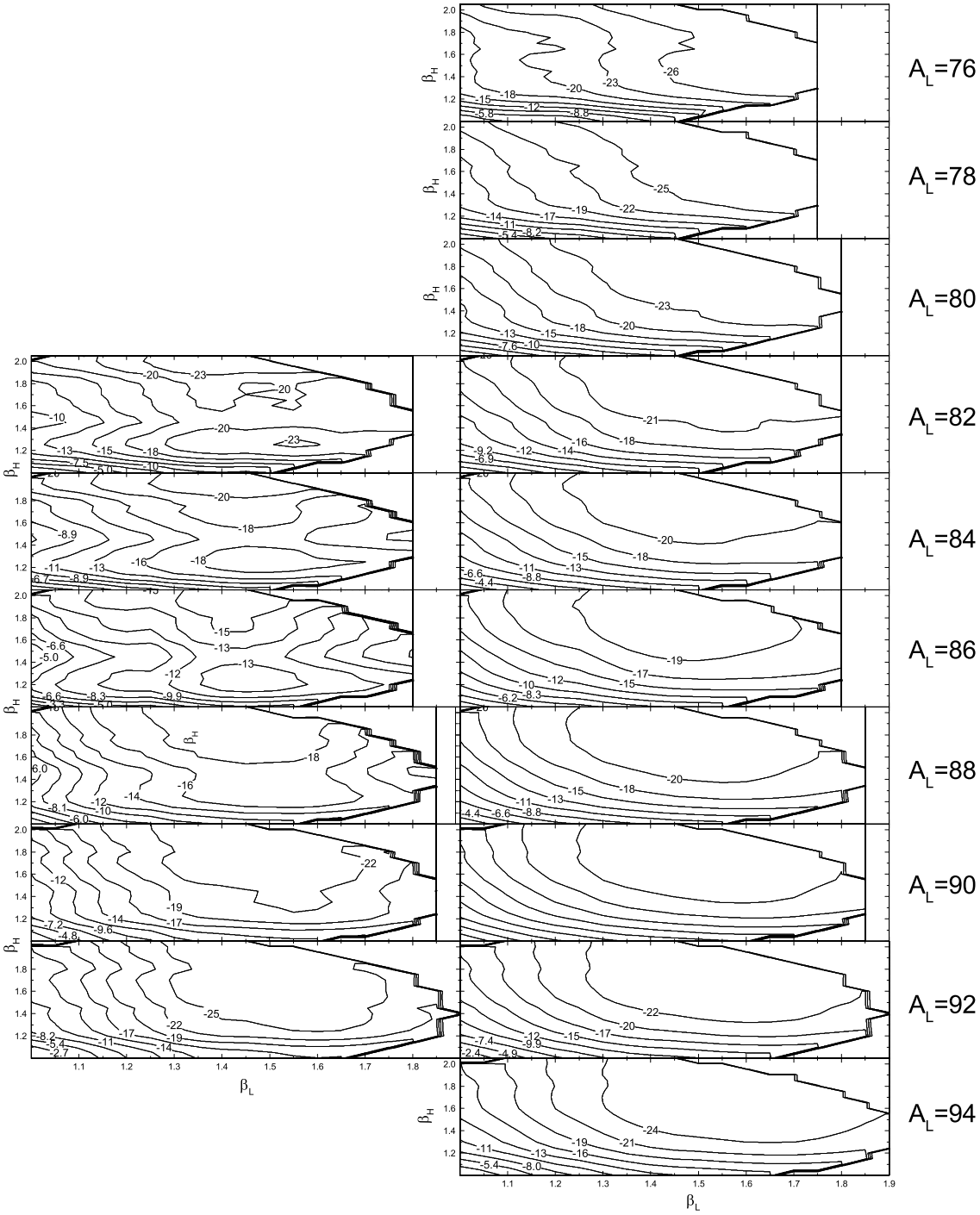
A_L=76
A_L=78
A_L=80
A_L=82
A_L=84
A_L=86
A_L=88
A_L=90
A_L=92
A_L=94
β_H
β_L

Discussions – High excitation energy of the CN

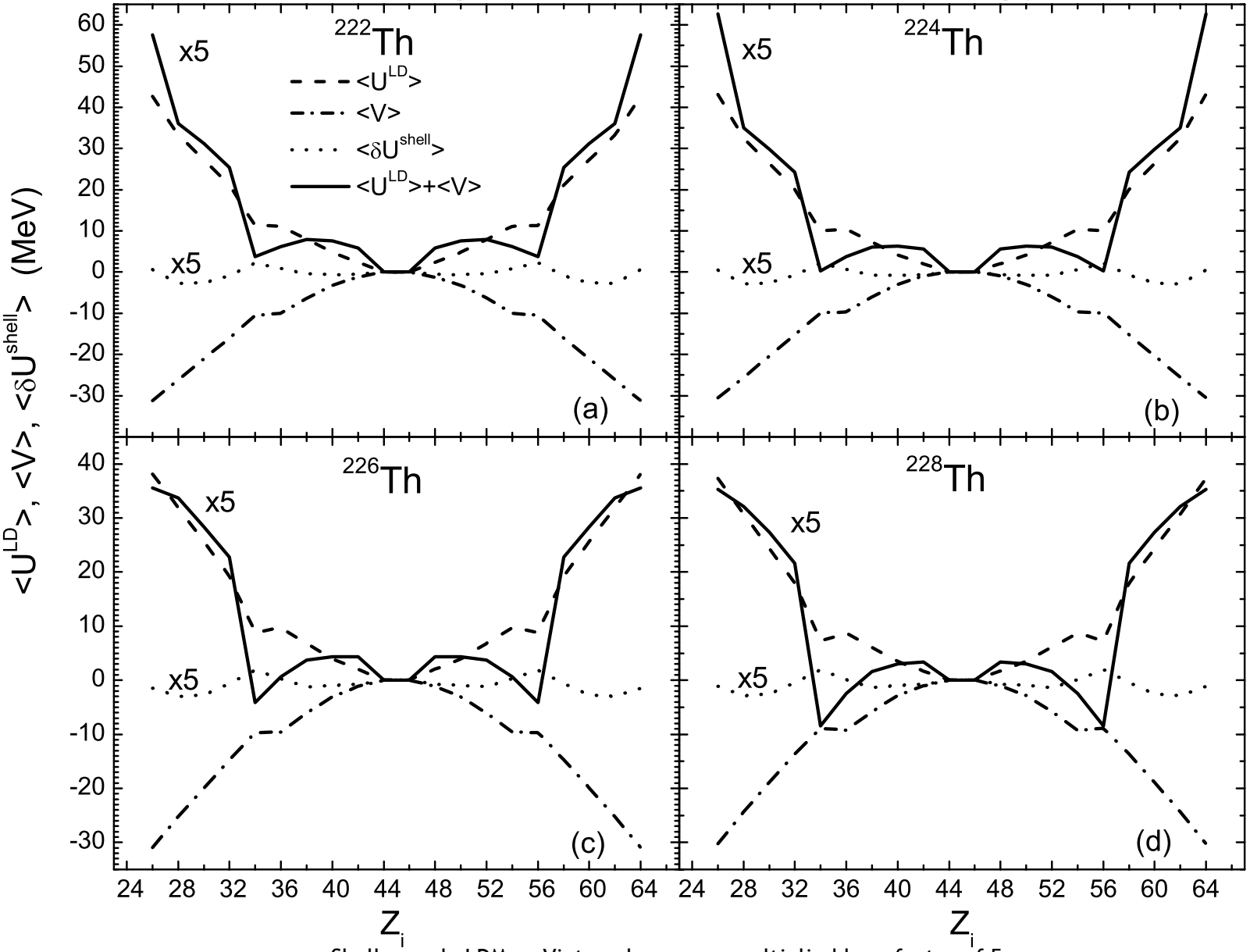

<Shells> and <LDM>+<Vint> values were multiplied by a factor of 5.

*H. Pașca, A.V. Andreev, G.G. Adamian, and N.V. Antonenko, Phys. Rev. C **94**, 064614 (2016)*
*H. Pașca, A.V. Andreev, G.G. Adamian, and N.V. Antonenko, Eur. Phys. J. A **52**, 369 (2016).*

Results

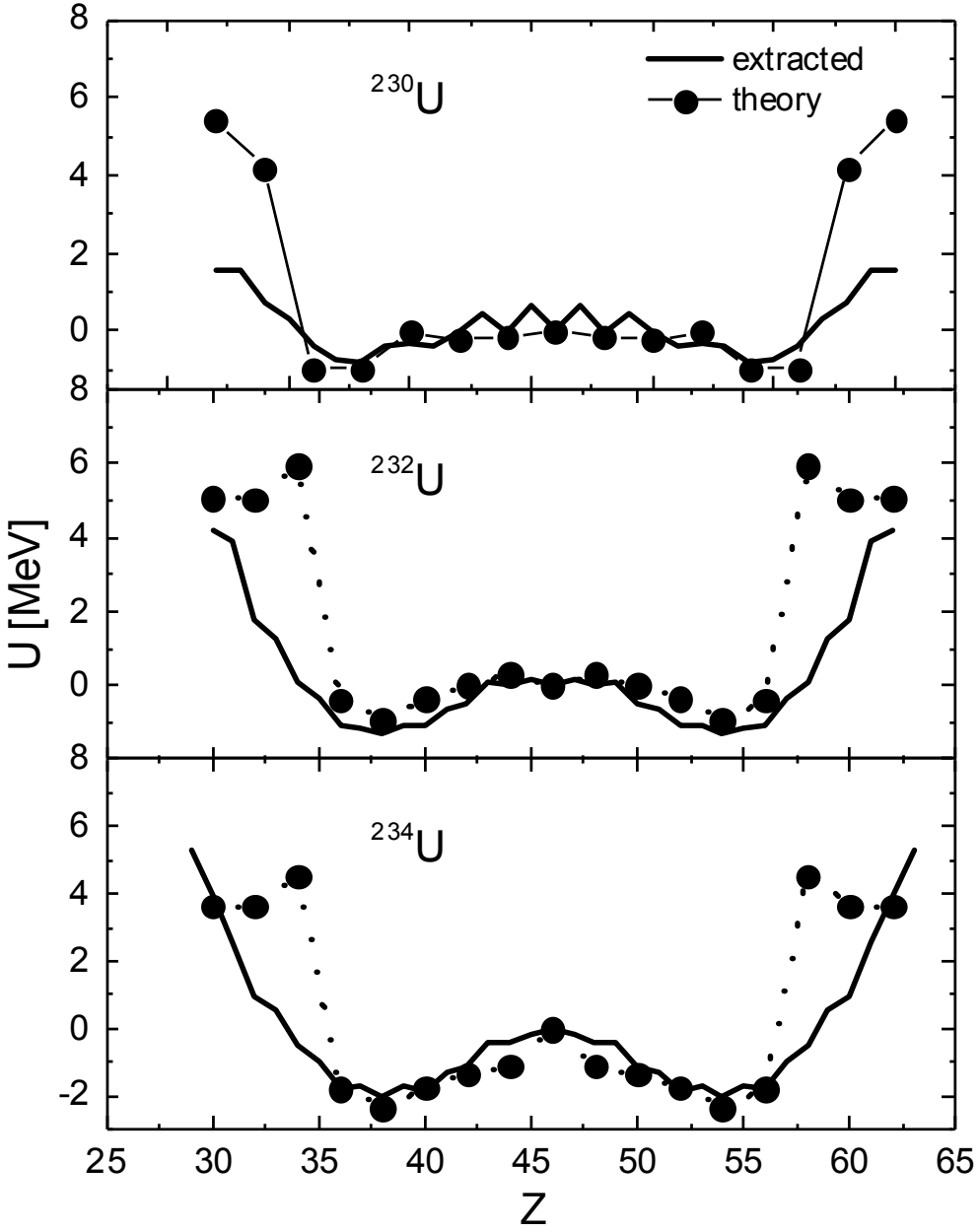

H. Pașca, A.V. Andreev, G.G. Adamian, and N.V. Antonenko, Eur. Phys. J. A ***52****, 369 (2016).*